Application of Repetitive Control to the Lateral Motion in a Roll-to-Roll Web System

by

Zhao Jin

A thesis
presented to the University of Waterloo
in fulfillment of the
thesis requirement for the degree of
Master of Mathematics
in
Applied Mathematics

Waterloo, Ontario, Canada, 2012

© Zhao Jin 2012

I hereby declare that I am the sole author of this thesis. This is a true copy of the thesis, including any required final revisions, as accepted by my examiners.

I understand that my thesis may be made electronically available to the public.

Abstract

In a roll-to-roll web system lateral motion of a web caused by disturbances, which are often periodic, results in poor product quality. To reduce the effect of such disturbances, two control strategies are applied. First, the internal model principle is used to reject a sinusoidal disturbance. Second, repetitive control theory is used to reject a general periodic disturbance. We provide the synthesis procedure for both strategies, and demonstrate its use in several simulation studies on a five-roller web system. The simulation results show that the effect of disturbances, either sinusoidal or triangular, on lateral motion are significantly reduced with the internal model controller or the modified repetitive controller.

Acknowledgements

I want to thank my advisor Professor Dong Eui Chang for mentoring me throughout my graduate studies. I have learned a great deal from him.

I want to also thank my thesis committee members Professor Xinzhi Liu and Professor Soo Jeon.

Thanks to Helen, Carol, Stephanie for answering my administration questions.

I want to thank my fellow office mates Jonathan, Boglarka, Wilten, Jared, and Zhaoxin. It has been fun these last two years. Also, thank you to everyone in the control group for all the interesting discussions and seminars.

Finally, I want to thank my family for their support.

Dedication

To The Simpsons, my favourite TV show.

Table of Contents

List of Tables

List of Figures

Chapter 1

Introduction

The term web is used to define a strip of continuous material where its length is much larger than its width. Webs describe many different types of material: paper, plastic, steel, fabrics and so on. A typical application involving webs is shown in Figure 1.1, where a web is released from a roll of material by the unwinder, transported around by rollers so that the material can be processed, and then accumulated into another roll of material by the rewinder. Such a system is called a roll-to-roll (RTR) web system or web processing line, and it has a wide range of applications in manufacturing such as mass production of metal products like aluminum or flexible electronics like solar cells. The study of web systems is essential for ensuring that webs do not break and product quality is consistent. Among several specifications, one specification is to eliminate the effect of the disturbance on lateral motion. Thus, the disturbance rejection problem for a web system serves as the motivation for this research.

1.1 Background

The web system shown in Figure 1.1 uses many rollers to transport the web in the longitudinal direction, the direction of transport. Among the rollers, there are the unwinder, the nip rollers, the guide rollers, and the rewinder. The unwinder, nip rollers, and rewinder are used to solve problems relating to web tension and velocity; see [1] for a survey. The guide rollers are used to solve problems relating to lateral motion, the motion in the plane of the web that is perpendicular to the longitudinal direction. The study of lateral motion is important, because it can cause a number of problems like web wrinkle, breaking of the

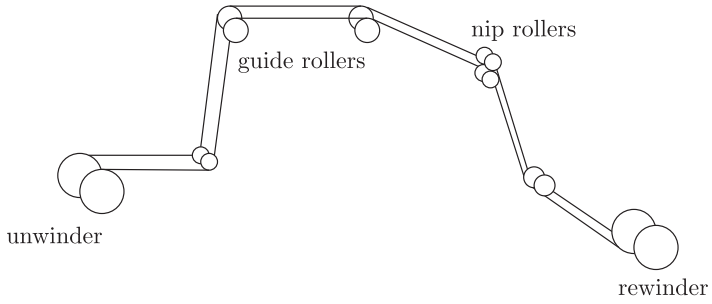

Figure 1.1: Web system.

web, inconsistent products, and low product quality. To ensure that these problems do not happen, the guide rollers are used to control the lateral motion.

The study of web lateral dynamics is achieved in three parts: first, modeling the lateral dynamics of the web; second, stabilizing the lateral motion, and third, rejecting any disturbances that affect lateral motion. The first two parts have been studied extensively. The third part is the main focus of this thesis.

The first major work in modeling web lateral dynamics was done by Shelton [2]. He used beam theory to model the lateral displacement of a web between two rollers. He then investigated the interaction between the web and a rotating roller in an effort to control the lateral motion. Subsequent works to improve the accuracy of his model were done in [3, 4, 5].

Based on the web lateral dynamics, researchers applied various control strategies to stabilize the lateral motion. A proportional controller was constructed in [3]. A lead-lag compensator was designed in [5]. A linear quadratic regulator (LQR) was synthesized in [6]. An observer-based feedback controller was constructed in [7]. In the series of papers, the main goals were to asymptotically stabilize the output or the full-state, and to meet some other performance specifications.

The disturbance rejection problem for web lateral dynamics has received little attention. Feedforward control was used to reject a deterministic sinusoidal disturbance [8]. Compared with proportional-integral control, feedforward control offered 50% reduction in steady-state lateral displacement in a simulation study. None of the past works have considered non-sinusoidal periodic disturbances.

Repetitive control theory has been developed for tracking periodic references or rejecting periodic disturbances or both. The main idea of the theory is to insert the model of the reference or disturbance into the controller, which is known as the internal model

principle [9]. The Laplace transform of a general periodic signal with period τ_d has infinite many poles at $j\frac{2\pi k}{\tau_d}$, $k = 0\ ,\ \pm 1,\ \cdots$. Therefore, a suggested internal model is $\frac{e^{-\tau_d s}}{1-e^{-\tau_d s}}$. However, stability of the closed-loop system cannot be achieved by adding this model into a feedback loop with a strictly proper plant. Hence, the modified repetitive controller (also called filtered repetitive controller) has been developed to overcome the stability problem [9]. Much improvements have been made in repetitive control theory, such as in performance [10], robustness [11, 12, 13], and capacity to reject multi-periodic disturbances [14]. Practical uses of repetitive control have been used for optical disk drives [11, 12] and cold rolling mills [14]. See [15] for a complete review of repetitive control theory and its applications.

1.2 Summary

The main contribution of this thesis is analyzing the disturbance rejection problem for the lateral motion of a roll-to-roll web system. In other words, we successfully apply the internal model controller presented in [16], the modified repetitive controller presented in [10], and the two period modified repetitive controller presented in [14] to reject certain disturbances that cause lateral motion in a RTR system.

The remainder of this thesis is organized as follows. In Chapter 2, the Timoshenko beam model for the lateral displacement of a web between two rollers is reviewed, and then the equations governing the lateral dynamics of the web and roller are derived. The model is extended to a five-roller web system. In Chapter 3, we look at existing works on the stabilization of lateral motion. In Chapter 4, we study the disturbance rejection problem for linear feedback systems. The theory of the internal model principle is studied for disturbances that are sinusoidal, and the theory of repetitive control is studied for general periodic disturbances. Synthesis procedures are given for each strategy. In Chapter 5, we synthesize an internal model controller and the modified repetitive controllers for a five-roller web system. Simulation results demonstrate that both strategies are effective in reducing the effect of the disturbance on the lateral motion. Chapter 6 contains the conclusions of the thesis.

Chapter 2

Web Lateral Dynamics

This chapter reviews a model of the lateral dynamics of a web between two rollers. Dynamics are obtained by first modeling the lateral displacement of the web using beam theory, and then analyzing the interaction of the web with a rotating roller. The model is then extended to the web between every two rollers in a five-roller web system. The state-space form of this system is proposed, and is shown to be both stabilizable and detectable.

2.1 Description of a Roll-to-Roll Web System

Roll-to-roll web systems like the one shown in Figure 2.1 are used in the mass production of flexible electronics. In the application, for example, a plastic web is transported by rollers through the web system and at some location, an electronic is printed onto the web.

In addition to transporting the web, active or driven rollers, such as a displacement guide aid in the control of lateral motion. Rollers R_1 and R_2 are the displacement guide, and it freely pivots about an axis parallel to the incoming web at roller R_1; see Figure 2.2 [3]. The idle or passive rollers R_0, R_3, and R_4 only provide transport for the web. A sensor is placed at roller R_0 to measure the the lateral displacement $y_0(t)$. Another sensor is placed at roller R_2 to measure the controlled output. Other properties of the system, such as distance between rollers, web properties, and operating conditions of the system is described in Table 1 of Appendix A.3.

The model of web lateral dynamics of this chapter is limited by the following assumptions [2, 3]:

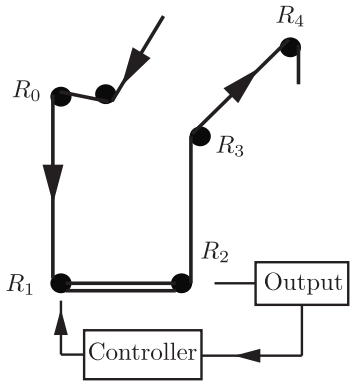

Figure 2.1: Web path.

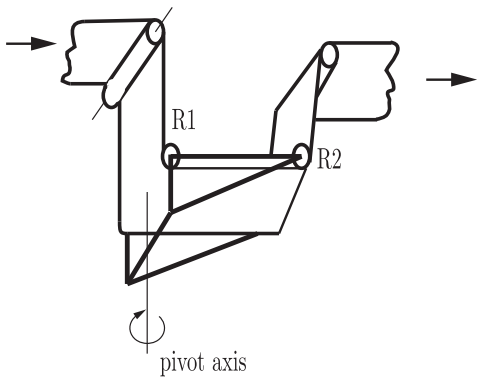

Figure 2.2: Displacement guide.

1. The contact area between the web and the roller is small in relation to the distance between two rollers.
2. Web velocity and tension are assumed to be constant or change slowly over time. Tension is so great that sagging of the web is small.
3. No web slippage.
4. All lateral displacements are small.
5. The web is homogeneous.
6. The length to width ratio of the web is relatively small. For example, less than a factor of ten.

2.2 Modeling Web Lateral Dynamics

The partial differential equation (PDE) that describes the lateral motion of the web is derived by treating the web as a Timoshenko beam experiencing tension in the direction

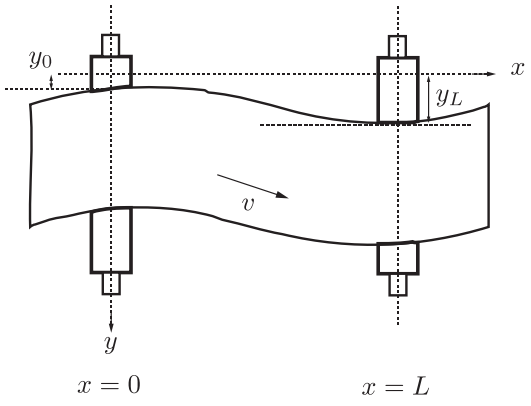

Figure 2.3: Web between two rollers

of transport. The fourth-order PDE that governs the lateral displacement $y(x,t)$ is

$$\begin{aligned} 0 = (Jv^2 - EI)\left(\frac{nmv^2}{GA} - \frac{nT}{GA} - 1\right)\frac{\partial^4 y}{\partial x^4} + (mv^2 - T)\frac{\partial^2 y}{\partial x^2} + 4mv\frac{\partial^2 y}{\partial x \partial t} + m\frac{\partial^2 y}{\partial t^2} \\ + \left(\frac{18Jnmv^2}{GA} - \frac{EInm}{GA} - \frac{JnT}{GA} - J\right)\frac{\partial^4 y}{\partial x^2 \partial t^2} + \frac{Jnm}{GA}\frac{\partial^4 y}{\partial t^4} + \frac{8Jnmv}{GA}\frac{\partial^4 y}{\partial x \partial t^3} \\ + \left(\frac{8Jnmv^3}{GA} - \frac{4EInmv}{GA} - \frac{4JnTv}{GA} - 4Jv\right)\frac{\partial^4 y}{\partial x^3 \partial t}; \end{aligned} \tag{2.1}$$

see Appendix A.1 for derivation of PDE. Equation (2.1) is simplified using three assumptions: 1) displacements and stresses do not change over time; that is, partial derivatives with respect to time are set to zero. This is called the quasistatic assumption, 2) $T \gg mv^2$; 3) $EI \gg Jv^2$. The simplified equation is

$$\frac{\partial^4 y(x,t)}{\partial x^4} - K^2\frac{\partial^2 y(x,t)}{\partial x^2} = 0, \tag{2.2}$$

where $K^2 = \frac{T}{EI\left(1+\frac{nT}{GA}\right)}$. The four boundary conditions for equation (2.2) are given as follows:

$$y(0,t) = y_0(t), \qquad \theta(0,t) = \frac{\partial y(0,t)}{\partial x} + \frac{EIn}{GA}\left(\frac{nT}{GA} + 1\right)\frac{\partial^3 y(0,t)}{\partial x^3} = \theta_0(t), \tag{2.3}$$

$$y(L,t) = y_L(t), \qquad \theta(L,t) = \frac{\partial y(L,t)}{\partial x} + \frac{EIn}{GA}\left(\frac{nT}{GA} + 1\right)\frac{\partial^3 y(L,t)}{\partial x^3} = \theta_L(t), \tag{2.4}$$

where $y_0(t)$ and $y_L(t)$ are respectively the lateral displacement of the web at $x = 0$ and $x = L$; see Figure 2.3, and $\theta_0(t)$ and $\theta_L(t)$ are respectively the angle of face rotation at $x = 0$ and $x = L$. The expression for the angle of face rotation is derived in Appendix A.1. Solving equation (2.2) with boundary conditions (2.3) and (2.4), we obtain the general solution:

$$y(x,t) = C_1(t)\sinh(Kx) + C_2(t)\cosh(Kx) + C_3(t)x + C_4(t), \tag{2.5}$$

where

$$\begin{aligned}
C_1(t) &= \frac{a\sinh(KL)}{R}\left(y_0(t) - y_L(t)\right) + \frac{[1-\cosh(KL)]}{KR}\left(\theta_0(t) - \theta_L(t)\right) + \frac{aL\sinh(KL)}{R}\theta_0(t),\\
C_2(t) &= \frac{a\left[1-\cosh(KL)\right]}{R}\left(y_0(t) - y_L(t)\right) + \frac{[\sinh(KL) - aKL\cosh(KL)]}{KR}\theta_0(t)\\
&\quad + \frac{[aKL - \sinh(KL)]}{KR}\theta_L(t),\\
C_3(t) &= \frac{a^2K\sinh(KL)}{R}\left(y_L(t) - y_0(t)\right) + \frac{a\left[1-\cosh(KL)\right]}{R}\left(\theta_0(t) + \theta_L(t)\right),\\
C_4(t) &= \frac{a\left[1-\cosh(KL)\right]}{R}\left(y_0(t) + y_L(t)\right) + \frac{a^2KL\sinh(KL)}{R}y_0(t)\\
&\quad - \frac{[\sinh(KL) - aKL\cosh(KL)]}{KR}\theta_0(t) - \frac{[aKL - \sinh(KL)]}{KR}\theta_L(t).
\end{aligned}$$

The variables a and R are defined as

$$a = 1 + K^2EI\frac{n}{GA}\left(1 + \frac{nT}{GA}\right), \tag{2.6}$$

$$R = a\left[2 - 2\cosh(KL)\right] + a^2KL\sinh(KL). \tag{2.7}$$

The lateral displacement of a web changes as the web approaches the second roller in Figure 2.3, because of the interaction between the roller and the web. The interaction is based on the property that a web approaching any given roller aligns itself perpendicular to the roller [2]. As a result, we can control the lateral displacement of the web y_L by rotating the roller. The lateral dynamics of y_L are

$$\begin{aligned}
\frac{dy_L}{dt} &= v\left(\gamma - \frac{\partial y_L}{\partial x}\right) + \frac{dz}{dt},\\
\frac{d^2y_L}{dt^2} &= v^2\frac{\partial^2 y_L}{\partial x^2} + \frac{d^2z}{dt^2},
\end{aligned}$$

where z and γ are respectively the lateral displacement and pivot angle of the guide roller, $\frac{\partial y_L}{\partial x}$ is the web slope and $\frac{\partial^2 y_L}{\partial x^2}$ is the web curvature at $x = L$. Both equations are derived below [2, 3].

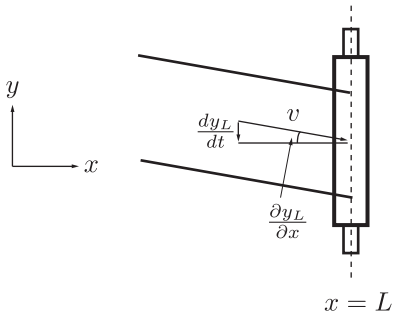

Figure 2.4: Roller at rest.

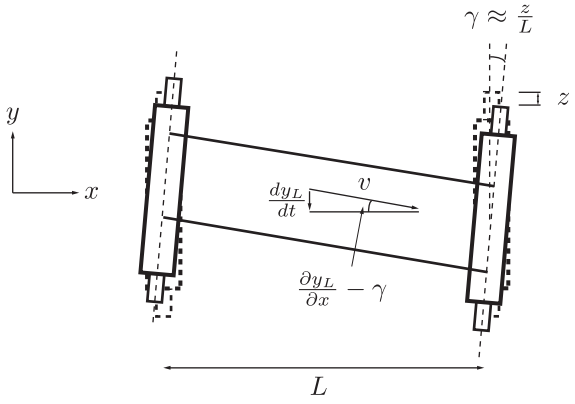

Figure 2.5: Roller is rotating.

2.2.1 Derivation of Web Lateral Velocity

We consider the contact position $x = L$ of the web and roller as shown in Figure 2.4. The constant web velocity is v, and the web slope is $\frac{\partial y_L}{\partial x}$ as the web makes contact with the roller. The lateral velocity of the web can be obtained by decomposing the velocity into its vector components. In other words, the lateral velocity, using the reference frame in the figure, is the velocity in the y-direction:

$$\frac{dy_L}{dt} = -v \sin\left(\frac{\partial y_L}{\partial x}\right) \approx -v\frac{\partial y_L}{\partial x}, \tag{2.8}$$

assuming web slope is small. The lateral velocity equation (2.8) is only valid when the roller is at rest. If the roller is rotating at an angle γ, and moving at a lateral velocity of $\frac{dz}{dt}$ as shown in Figure 2.5, then the lateral velocity of the web, using the same reference frame, is the velocity in the y-direction plus the lateral velocity of the roller:

$$\frac{dy_L}{dt} = -v \sin\left(\frac{\partial y_L}{\partial x} - \gamma\right) + \frac{dz}{dt} \approx v\left(\gamma - \frac{\partial y_L}{\partial x}\right) + \frac{dz}{dt}, \tag{2.9}$$

assuming web slope and pivot angles are small. Furthermore, we use the approximation $\gamma \approx \frac{z}{L}$ to simplify equation (2.9) to the following

$$\frac{dy_L}{dt} = v\left(\frac{z}{L} - \frac{\partial y_L}{\partial x}\right) + \frac{dz}{dt}. \tag{2.10}$$

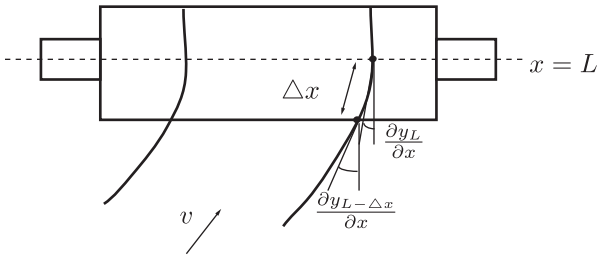

Figure 2.6: Lateral acceleration of the web at the location of $x = L$.

2.2.2 Derivation of Web Lateral Acceleration

We consider the contact position $x = L$ of the web and roller as shown in Figure 2.6. The constant web velocity is v, the web slope at the contact position is $\frac{\partial y_L}{\partial x}$, and the web slope at $\triangle x$ before the contact position is $\frac{\partial y_{L-\triangle x}}{\partial x}$. The lateral acceleration of the web is derived by considering the change in web velocity v from the point $x = L - \triangle x$ to the point $x = L$:

$$\frac{\triangle v}{\triangle t} = \frac{v_L - v_{L-\triangle x}}{\triangle t}. \tag{2.11}$$

We use the Tyalor approximation of $v_{L-\triangle x}$ at $x = L$ and take the limit as $\triangle t \to 0$:

$$\begin{aligned}
\frac{d^2 y_L}{dt^2} = \lim_{\triangle t \to 0} \frac{\triangle v}{\triangle t} &= \frac{-v\frac{\partial y_L}{\partial x} + v\left(\frac{\partial y_L}{\partial x} + \triangle x \frac{\partial^2 y_L}{\partial x^2} + O\left((\triangle x)^2\right)\right)}{\triangle t} \\
&= \lim_{\triangle t \to 0} \left[v \frac{\triangle x}{\triangle t} \frac{\partial^2 y_L}{\partial x^2} + \frac{\triangle x}{\triangle t} O(\triangle x) \right] \qquad (2.12) \\
&= v^2 \frac{\partial^2 y_L}{\partial x^2}. \qquad (2.13)
\end{aligned}$$

To obtain equation (2.13) from (2.12), we use $\frac{\triangle x}{\triangle t} \to v$ as $\triangle t \to 0$, and ignore terms of $O(\triangle x)$. The lateral acceleration equation (2.13) considers the roller at rest. If the roller is moving with lateral acceleration $\frac{d^2 z}{dt^2}$, then equation (2.13) becomes

$$\frac{d^2 y_L}{dt^2} = v^2 \frac{\partial^2 y_L}{\partial x^2} + \frac{d^2 z}{dt^2}. \tag{2.14}$$

The combination of lateral velocity (2.10), and lateral acceleration (2.14) governs the lateral dynamics of y_L. In order to compute $\frac{\partial y_L}{\partial x}$ and $\frac{\partial^2 y_L}{\partial x^2}$ easily, we change the form of the general solution (2.5) into a more convenient form:

$$y(x,t) = y_0(t)X_1(x) + \theta_0(t)X_2(x) + y_L(t)X_3(x) + \theta_L(t)X_4(x), \tag{2.15}$$

with

$$
\begin{aligned}
X_1(x) = \{ & a\sinh(KL)\sinh(Kx) + a\left[1-\cosh(KL)\right]\cosh(Kx) \\
& - a^2\sinh(KL)Kx + a^2KL\sinh(KL) \\
& + a\left[1-\cosh(KL)\right]\}/R, \\
X_2(x) = \{ & \left[1-\cosh(KL) + aKL\sinh(KL)\right]\sinh(Kx) \\
& + \left[\sinh(KL) - aKL\cosh(KL)\right]\cosh(Kx) \\
& + a\left[1-\cosh(KL)\right]Kx \\
& - \left[\sinh(KL) - aKL\cosh(KL)\right]\}/KR, \\
X_3(x) = \{ & -a\sinh(KL)\sinh(Kx) \\
& - a\left[1-\cosh(KL)\right]\cosh(Kx) \\
& + a^2\sinh(KL)Kx + a\left[1-\cosh(KL)\right]\}/R, \\
X_4(x) = \{ & -\left[1-\cosh(KL)\right]\sinh(Kx) + a\left[1-\cosh(KL)\right]Kx \\
& + \left[aKL - \sinh(KL)\right]\cosh(Kx) \\
& - \left[aKL - \sinh(KL)\right]\}/KR,
\end{aligned}
\tag{2.16}
$$

where a and R are respectively defined by equations (2.6) and (2.7). Now, the expressions for the slope and curvature of the web are obtained by differentiating the solution (2.15) with respect to x and evaluating it at $x = L$:

$$
\begin{aligned}
\frac{\partial y_L}{\partial x} &= y_0(t)X_1'(L) + \theta_0(t)X_2'(L) + y_L(t)X_3'(L) + \theta_L(t)X_4'(L), \\
\frac{\partial^2 y_L}{\partial x^2} &= y_0(t)X_1''(L) + \theta_0(t)X_2''(L) + y_L(t)X_3''(L) + \theta_L(t)X_4''(L).
\end{aligned}
$$

2.3 Extension to the Five-Roller Web System

We consider the five-roller web system shown in Figure 2.7. Let the superscript u denote the upstream contact point of the roller and the superscript d denote the downstream contact point of the roller. For example, $y_1^u(t)$ is the lateral displacement of the web upstream of roller R_1. The lateral displacement of web, $y(x,t)$, between every pair of rollers in Figure 2.7 is modeled using beam theory. In other words, we solve the PDE (2.2) for the boundary

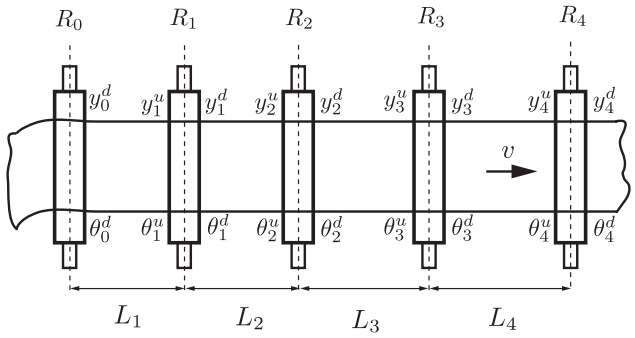

Figure 2.7: Lateral displacement and face rotation upstream and downstream of the rollers.

conditions:

$$R_0 - R_1 : y(0,t) = y_0^d(t), \quad \theta(0,t) = \theta_0^d(t), \quad y(L_1,t) = y_1^u, \quad \theta(L_1,t) = \theta_1^u, \tag{2.17}$$
$$R_1 - R_2 : y(0,t) = y_1^d(t), \quad \theta(0,t) = \theta_1^d(t), \quad y(L_2,t) = y_2^u, \quad \theta(L_2,t) = \theta_2^u, \tag{2.18}$$
$$R_2 - R_3 : y(0,t) = y_2^d(t), \quad \theta(0,t) = \theta_2^d(t), \quad y(L_3,t) = y_3^u, \quad \theta(L_3,t) = \theta_3^u, \tag{2.19}$$
$$R_3 - R_4 : y(0,t) = y_3^d(t), \quad \theta(0,t) = \theta_3^d(t), \quad y(L_4,t) = y_4^u, \quad \theta(L_4,t) = \theta_4^u. \tag{2.20}$$

At the rollers, two matching conditions for the joining web segments are necessary for simplifying the boundary conditions (2.17) to (2.20). The following approximations for the matching conditions are used:

$$y_i^u \approx y_i^d = y_i, \tag{2.21}$$
$$\theta_i^u \approx \theta_i^d = \theta_i. \tag{2.22}$$

These approximations are valid if the roller radius is much less than roller spacing [3]. Using matching conditions (2.21) and (2.22), the simplified boundary conditions are

$$y(0,t) = y_{i-1}(t), \quad \theta(0,t) = \theta_{i-1}(t), \quad y(L_i,t) = y_i(t), \quad \theta(L_i,t) = \theta_i(t), \tag{2.23}$$

for $i = 1 \ldots 4$, where $y_i(t)$ is the lateral displacement, and $\theta_i(t)$ is the angle of face rotation at roller R_i. The set of solutions are given in the convenient form:

$$y(x,t) = y_{i-1}(t)X_1(x) + \theta_{i-1}(t)X_2(x) + y_i(t)X_3(x) + \theta_i(t)X_4(x), \quad i = 1, \ldots, 4, \tag{2.24}$$

where $X_1(x)$, $X_2(x)$, $X_3(x)$, $X_4(x)$ are defined in equation (2.16).

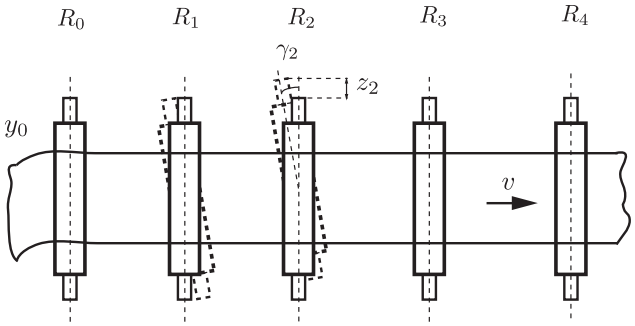

Figure 2.8: Schematic view of the five-roller web system.

We extend the lateral dynamics (2.10) and (2.14) to rollers R_1, R_2, R_3, and R_4 with rollers R_1–R_2 as a displacement guide; see Figure 2.8. As a result, we obtain eight equations:

$$\frac{dy_1}{dt} = -v\frac{\partial y_1}{\partial x}, \tag{2.25}$$

$$\frac{d^2y_1}{dt^2} = v^2\frac{\partial^2 y_1}{\partial x^2}, \tag{2.26}$$

$$\frac{dy_2}{dt} = v\left(\frac{z_2}{L_2} - \frac{\partial y_2}{\partial x}\right) + \frac{dz_2}{dt}, \tag{2.27}$$

$$\frac{d^2y_2}{dt^2} = v^2\frac{\partial^2 y_2}{\partial x^2} + \frac{d^2z_2}{dt^2}, \tag{2.28}$$

$$\frac{dy_3}{dt} = -v\frac{\partial y_3}{\partial x}, \tag{2.29}$$

$$\frac{d^2y_3}{dt^2} = v^2\frac{\partial^2 y_3}{\partial x^2}, \tag{2.30}$$

$$\frac{dy_4}{dt} = -v\frac{\partial y_4}{\partial x}, \tag{2.31}$$

$$\frac{d^2y_4}{dt^2} = v^2\frac{\partial^2 y_4}{\partial x^2}. \tag{2.32}$$

Note that the pivot angle, lateral velocity, and acceleration of the rollers are zero except for the the displacement guide.

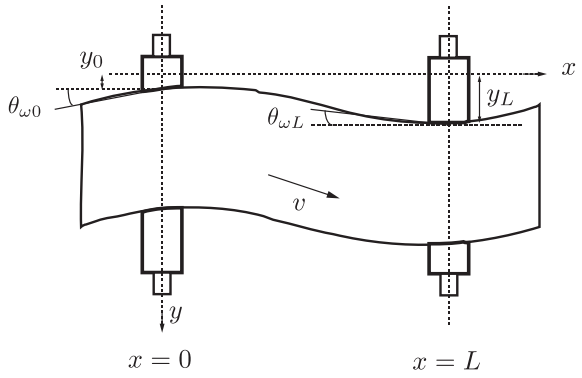

Figure 2.9: Boundary conditions.

2.4 Other Lateral Dynamics Models

This section briefly reviews two other beam models for describing web lateral dynamics.

2.4.1 Euler-Bernoulli Beam

If the web is described as a static beam under tension with negligible mass, then the following PDE governs the lateral displacement $y(x,t)$:

$$\frac{\partial^4 y(x,t)}{\partial x^4} - K^2 \frac{\partial^2 y(x,t)}{\partial x^2} = 0,$$

where $K^2 = \frac{T}{EI}$. The four boundary conditions are a result of the web lateral displacement, and angle of entry of the web as it approaches the two rollers:

$$y(0,t) = y_0(t), \qquad \frac{\partial y(0,t)}{\partial x} = \theta_{\omega 0}(t), \tag{2.33}$$

$$y(L,t) = y_L(t), \qquad \frac{\partial y(L,t)}{\partial x} = \theta_{\omega L}(t), \tag{2.34}$$

where $y_0(t)$ and $y_L(t)$ are the lateral displacement, and $\theta_{\omega 0}(t)$ and $\theta_{\omega L}(t)$ are the angle of entry of the web on the rollers; see Figure 2.9. The general solution is of the same form of solution (2.5) with different $C_i(t)$, for $i = 1, 2, 3, 4$ [2, 6].

2.4.2 Timoshenko Beam

This model has been studied in detail in the previous sections.

2.4.3 Euler-Bernoulli Beam with Viscoelasticity

If web viscoelasticity is considered, then the following PDE governs the lateral displacement $y(x,t)$:

$$EI\frac{\partial^4 y(x,t)}{\partial x^4} - T\frac{\partial^2 y(x,t)}{\partial x^2} + \eta I\frac{\partial^5 y}{\partial x^4 \partial t} + m\frac{\partial^2 y}{\partial t^2} = 0$$

where η is the viscosity of the material [5]. The numerical solution is computed using a finite-difference scheme with the same boundary conditions (2.33) and (2.34).

The Timoshenko model is an improvement to the E-B model, because it considers the shear deformation. As a consequence, the boundary conditions and the constant K for the PDE are different. Sievers states this improvement is necessary if the the ratio of the length to width is less than a factor of ten [3]. On the other hand, the need for adding the viscoelastic term to the E-B model depends the web material used. For example, viscosity of the material is important for rubber or paper webs [5]. If viscosity and shear deformation are not important factors, then the simple E-B beam model is suitable at describing the web lateral dynamics.

2.5 State-Space Form of the System Dynamics

We put the system dynamics (2.25) to (2.32) in state-space form:

$$\begin{aligned} \dot{x}(t) &= Ax(t) + Bu(t) + Fw(t) \\ y(t) &= Cx(t), \end{aligned} \tag{2.35}$$

where the state $x(t)$, the output $y(t)$, the control input $u(t)$, and the disturbance or exogenous input $w(t)$ are given respectively by

$$x = \begin{bmatrix} y_1 & \frac{dy_1}{dt} & y_2 & \frac{dy_2}{dt} & y_3 & \frac{dy_3}{dt} & y_4 & \frac{dy_4}{dt} & z_2 & \frac{dz_2}{dt} \end{bmatrix}^T,$$

$$y(t) = y_2(t), \qquad u(t) = \frac{d^2 z_2(t)}{dt^2}, \qquad w(t) = \begin{bmatrix} y_0(t) & \theta_0(t) \end{bmatrix}^T.$$

The matrices A, B, C, and F are given as follows:

$$A = \begin{bmatrix} 0 & 1 & 0 & 0 & 0 & 0 & 0 & 0 & 0 & 0 \\ a_{21} & a_{22} & 0 & 0 & 0 & 0 & 0 & 0 & 0 & 0 \\ 0 & 0 & 0 & 1 & 0 & 0 & 0 & 0 & 0 & 0 \\ a_{41} & a_{42} & a_{43} & a_{44} & 0 & 0 & 0 & 0 & a_{49} & a_{4,10} \\ 0 & 0 & 0 & 0 & 0 & 1 & 0 & 0 & 0 & 0 \\ a_{61} & a_{62} & a_{63} & a_{64} & a_{65} & a_{66} & 0 & 0 & a_{69} & a_{6,10} \\ 0 & 0 & 0 & 0 & 0 & 0 & 0 & 1 & 0 & 0 \\ a_{81} & a_{82} & a_{83} & a_{84} & a_{85} & a_{86} & a_{87} & a_{88} & a_{89} & a_{8,10} \\ 0 & 0 & 0 & 0 & 0 & 0 & 0 & 0 & 0 & 1 \\ 0 & 0 & 0 & 0 & 0 & 0 & 0 & 0 & 0 & 0 \end{bmatrix}, \tag{2.36}$$

$$B = \begin{bmatrix} 0 & 0 & 1 & 0 & 0 & 0 & 0 & 0 & 0 & 1 \end{bmatrix}^T, \tag{2.37}$$

$$C = \begin{bmatrix} 0 & 0 & 1 & 0 & 0 & 0 & 0 & 0 & 0 & 0 \end{bmatrix}, \tag{2.38}$$

$$F = \begin{bmatrix} 0 & f_{21} & 0 & f_{41} & 0 & f_{61} & 0 & f_{81} & 0 & 0 \\ 0 & f_{22} & 0 & f_{42} & 0 & f_{62} & 0 & f_{82} & 0 & 0 \end{bmatrix}^T; \tag{2.39}$$

see Appendix A.2 for derivation of the expressions in matrices A and F. The disturbance $w(t)$ has two components: $y_0(t)$ and $\theta_0(t)$. The first component $y_0(t)$ is caused by the combination of web camber, method of web formation, and interaction of web with machine parts [3]. It is measured by a sensor placed at roller R_0. We provide two experimental examples from literature of $y_0(t)$, and its effect on the lateral displacement; see Figure 2.10 for the five-roller web system [4], and see Figure 2.11 for the system described in [6]. We see that $y_0(t)$ can be described by an approximate sinusoidal wave or a periodic function. The second component $\theta_0(t)$ cannot be measured [4]. However, for the remainder of the thesis, it is assumed to be negligible; that is, set it to zero. We evaluate the expressions in

A and F with values in Table 2 of Appendix A.3 and set $\theta_0(t)$ to zero:

$$A = \begin{bmatrix} 0 & 1.0 & 0 & 0 & 0 & 0 & 0 & 0 & 0 & 0 \\ -5.4 & -3.4 & 0 & 0 & 0 & 0 & 0 & 0 & 0 & 0 \\ 0 & 0 & 0 & 1.0 & 0 & 0 & 0 & 0 & 0 & 0 \\ 7.3 & -0.9 & -8.4 & -4.1 & 0 & 0 & 0 & 0 & 8.4 & 4.1 \\ 0 & 0 & 0 & 0 & 0 & 1.0 & 0 & 0 & 0 & 0 \\ 0.9 & -1.1 & 1.2 & -1.3 & -3.4 & -2.7 & 0 & 0 & 2.1 & 1.3 \\ 0 & 0 & 0 & 0 & 0 & 0 & 0 & 1.0 & 0 & 0 \\ 0.6 & -0.7 & 1.0 & -0.9 & -0.9 & -1.2 & -1.8 & -2.0 & 1.5 & 0.9 \\ 0 & 0 & 0 & 0 & 0 & 0 & 0 & 0 & 0 & 1.0 \\ 0 & 0 & 0 & 0 & 0 & 0 & 0 & 0 & 0 & 0 \end{bmatrix},$$

$$F = \begin{bmatrix} 0 & 5.4 & 0 & 1.1 & 0 & 1.3 & 0 & 0.9 & 0 & 0 \end{bmatrix}^T,$$

$$w(t) = y_0(t).$$

Before control design, we examine the stabilizability and detectability of the system. We refer the reader to Chapter 6 of [16] for definitions and theorems relating to controllability, stabilizability, observability, and detectability.

First, we check for controllability of the pair (A, B) by computing the rank of the controllability matrix for (A, B):

$$\operatorname{rank} \begin{bmatrix} B & AB & \cdots & A^9B \end{bmatrix} = 6.$$

Since the controllability matrix is not of full rank, the pair (A, B) is not controllable. However, there is a similarity transformation

$$A_1 = P_1 A P_1^{-1}, \;\; B_1 = P_1 B,$$

such that (A, B) is decomposed into its uncontrollable part, $(A_{uc}, 0_{4\times 1})$ of dimension 4 and controllable part (A_c, B_c) of dimension 6

$$A_1 = \begin{bmatrix} A_{uc} & 0 \\ A_{21} & A_c \end{bmatrix}, \;\; B_1 = \begin{bmatrix} 0 \\ B_c \end{bmatrix}.$$

The dynamics of the uncontrollable subsystem is verified to be exponentially stable; see the uncontrollable modes in Table 2.1. The system is said to be stabilizable. Second, we check for observability of the pair (C, A) by computing the rank of the observability matrix for (C, A):

$$\operatorname{rank} \begin{bmatrix} C^T & A^TC^T & \cdots & (A^T)^9C^T \end{bmatrix} = 6.$$

Since the observability matrix is not of full rank, the pair (C, A) is not observable. However, there is a similarity transformation

$$A_2 = P_2 A P_2^{-1}, \;\; C_2 = C P_2^{-1},$$

such that (C, A) is decomposed into its unobservable part, $(0_{1\times 4}, A_{no})$ of dimension 4 and its observable part (C_o, A_o) of dimension 6

$$A_2 = \begin{bmatrix} A_{no} & A_{12} \\ 0 & A_o \end{bmatrix}, \;\; C_2 = \begin{bmatrix} 0 & C_o \end{bmatrix}.$$

The dynamics of the unobservable part is verified to be exponentially stable; see the unobservable modes in Table 2.1. Hence, the system (2.35) is both stabilizable and detectable. These two properties allow us to design an observer-based feedback controller.

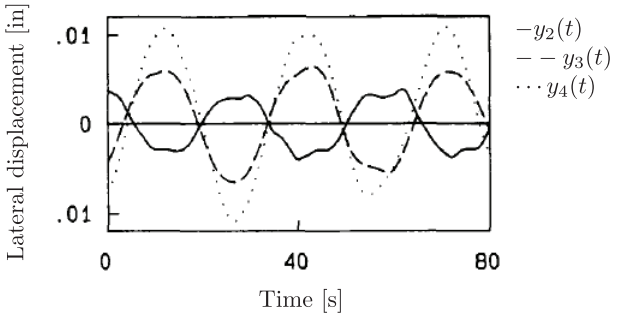

Figure 2.10: Effect of a periodic disturbance on lateral displacement.

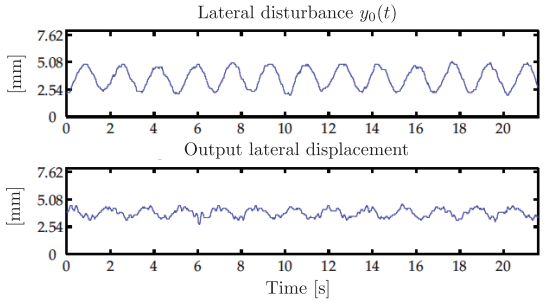

Figure 2.11: Disturbance and its effect on lateral displacement.

Table 2.1: Uncontrollable modes and unobservable modes

Uncontrollable modes	–2.07 + j2.03 –2.07 – j2.03	–1.67 + j1.62 –1.67 – j1.62
Unobservable modes	–1.34 + j1.25 –1.34 – j1.25	–1.01 + j0.88 –1.01 – j0.88

Chapter 3

Control of Lateral Motion

In this chapter, we review existing works on the stabilization of lateral motion in a roll-to-roll web system. The focus has been to use linear control strategies to control the lateral displacement of the web.

3.1 Proportional-Integral-Derivative (PID) Control

PID is among the first control strategy used because of its simplicity. The system dynamics (2.35) are changed into an equivalent unity feedback control form and then the gains, such as the proportional gains are tuned for performance [3]. The drawback of this method is that if the proportional gains are significantly increased, the feedback system may become unstable.

3.2 Observer-Based Feedback Control

An observer-based feedback controller offers an improvement to PID control for system (2.35), because the full-state, not only the output, are stabilized. The stabilizability and detectability of the system (see Chapter 2) allows us to design a controller, and a Luenberger observer so that the full state is stabilized using dynamic output feedback. This procedure is a standard pole-placement problem that can be found in [17].

3.3 Linear-Quadratic Regulator (LQR)

In [6], an LQR is used and its performance is evaluated under different operating conditions, such as changes in web tension and velocity. A reason for using optimal control is that the designer may not know the desirable closed-loop pole locations. For example, choosing pole locations far from the origin may give fast dynamic response, but require large gains that exceed physical limitations. In such cases, the closed-loop behavior may not behave as intended. Therefore, optimal control serves as a good initial design for a system [17].

3.4 Lead-Lag Compensator

A lead-lag compensator (3.1) is designed to control the lateral motion by analyzing the sensitivity function [5]. The lead-lag compensator has the form:

$$G\left(\frac{s+z_1}{s+p_1}\right)\left(\frac{s+z_2}{s+p_2}\right), \tag{3.1}$$

where G is a constant gain, z_1, z_2 are the zeros, and p_1, p_2 are the poles. Lead-lag compensation is a classic control tool that is useful for lowering the high-frequency gain, improving steady-state error, and improving transient response [18].

3.5 Feedforward Control

The feedforward control structure in Figure 3.1 for a web system under the influence of a known sinusoidal disturbance is studied in [8]. The objective of this study is to use PID control to stabilize the lateral displacement without disturbance, and then use the feedforward controller to reduce the effect of the disturbance. Their simulation results showed 50% improvement in reduction of lateral displacement compared to PID control [8].

The control objective of existing works have been to stabilize the lateral motion, but none have focused on the disturbance rejection problem with the exception of [8]. We see in the next chapter that if the disturbance can be accurately approximated by a sinusoidal wave, then we can completely eliminate it by using the well known internal model principle. However, if the disturbance is not sinusoidal but periodic, then we can use the repetitive control strategy to reduce the effect of the disturbance on lateral motion.

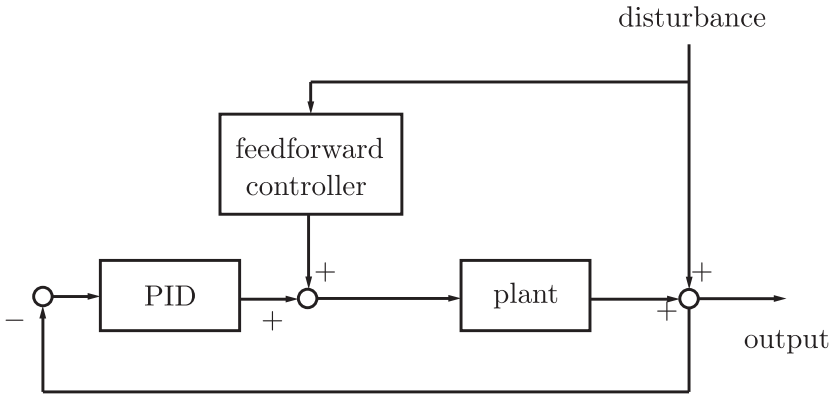

Figure 3.1: Feedforward control structure.

Chapter 4

Disturbance Rejection

In this chapter, we study the disturbance rejection problem for the closed-loop system considered in Figure 4.1. Given the plant transfer function $P(s)$ and the disturbance $d(t)$, the problem is to find a controller $\mathcal{C}(s)$ so that the feedback system is asymptotically stable and meets other specifications. One important specification is to require the effect of the disturbance signal $d(t)$ to approach zero as $t \to \infty$; that is, $y(t) \to 0$ as $t \to \infty$. This is called asymptotic or perfect disturbance rejection. However, for certain disturbances, asymptotic disturbance rejection may be unrealistic to achieve, so in these cases we require that the output $y(t)$ to remain bounded. This is called disturbance rejection. The disturbance rejection problem is studied for disturbances that are sinusoidal functions with known periods in Section 4.1, and general periodic functions with known periods in Sections 4.2, 4.3, 4.4.

4.1 Internal Model Principle

We consider a sinusoidal disturbance $d(t)$ with a known period in the closed-loop system shown in Figure 4.2, where $D(s)$, $Y(s)$, $R(s)$ are respectively the Laplace transform of $d(t)$, $y(t)$, $r(t)$. To achieve asymptotic disturbance rejection for the feedback system, the controller $\mathcal{C}(s)$ must contain a model of the disturbance [19]. This strategy is known as the internal model principle, which is stated more formally by the next theorem.

Theorem 1 (Theorem 9.3 [16]). *Consider the feedback system shown in Figure 4.2 with a strictly proper plant $P(s) = \frac{N_p(s)}{D_p(s)}$. It is assumed $D_p(s)$ and $N_p(s)$ are co-prime. The disturbance is modeled as $D(s) = \frac{N_d(s)}{D_d(s)}$. Let $\phi(s)$ be the unstable poles of $D(s)$. If no roots*

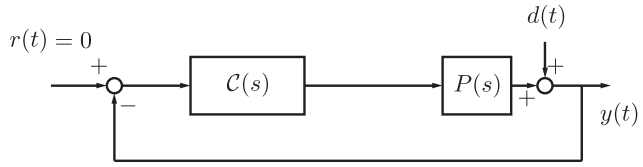

Figure 4.1: General closed-loop system.

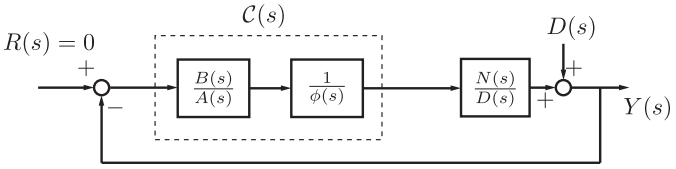

Figure 4.2: Closed-loop system with an internal model.

of $\phi(s)$ is a zero of $P(s)$, then there exists a proper controller $K(s) = \frac{B(s)}{A(s)}$ such that the overall system will reject $d(t)$, both asymptotically and robustly.

If no roots of $\phi(s)$ is a zero of $P(s)$, then $\tilde{D}(s) = D_p(s)\phi(s)$ and $N_p(s)$ are coprime. This means that there exists a proper controller $K(s) = \frac{B(s)}{A(s)}$ such that the polynomial $F(s)$ in

$$F(s) = A(s)\tilde{D}(s) + B(s)N_p(s) \tag{4.1}$$

has any desired roots (Theorem 9.1 [16]). We choose

$$\mathcal{C}(s) = \frac{B(s)}{A(s)\phi(s)}, \tag{4.2}$$

as shown in Figure 4.2, to achieve the design. Let us compute the transfer function from $D(s)$ to $Y(s)$:

$$\begin{aligned} Y(s) &= D(s) + \mathcal{C}(s)P(s)\left(-Y(s)\right), \\ Y(s) &= \frac{1}{1 + \mathcal{C}(s)P(s)} D(s). \end{aligned} \tag{4.3}$$

By using equations for $D(s)$, $\mathcal{C}(s)$, and $P(s)$, equation (4.3) becomes

$$
\begin{aligned}
Y(s) &= \frac{1}{1+\frac{N_p(s)B(s)}{D_p(s)A(s)\phi(s)}}\frac{N_d(s)}{D_d(s)} \\
Y(s) &= \frac{A(s)D_p(s)\phi(s)}{A(s)D_p(s)\phi(s)+N_p(s)B(s)}\frac{N_d(s)}{D_d(s)} \\
Y(s) &= \frac{D_p(s)A(s)N_d(s)}{F(s)}\frac{\phi(s)}{D_d(s)} \qquad (4.4)
\end{aligned}
$$

Because all the unstable poles of $D(s)$ are canceled by $\phi(s)$, the poles of $Y(s)$ can be assigned to have negative real parts. Thus, the system achieves asymptotic disturbance rejection; $y(t) \to 0$ as $t \to \infty$. In addition, we see that even if $N_p(s)$, $D_p(s)$, $B(s)$ and $A(s)$ change, as long as the overall system remains stable, and the unstable poles of the disturbance $D(s)$ are canceled by $\phi(s)$, the system will achieve asymptotic disturbance rejection. Therefore, the design is robust.

The procedure for synthesizing $\mathcal{C}(s)$ consists of two steps. First, we insert the model $\frac{1}{\phi(s)}$ of the disturbance signal inside the loop. Second, we carry out the pole-placement problem for $F(s)$. The details of the procedure for a sinusoidal disturbance are given below [16].

S1: Insert the internal model $\frac{1}{\phi(s)} = \frac{1}{s^2+\omega_d^2}$ inside the loop, where $T = \frac{2\pi}{\omega_d}$ is the known period of the sinusoidal disturbance.

S2: Carry out the pole-placement problem for a desired $F(s)$:

$$
F(s) = A(s)\tilde{D}(s) + B(s)N_p(s), \qquad \tilde{D}(s) = D_p(s)\phi(s), \qquad (4.5)
$$

S2a: Assume $\deg N_p(s) < \deg \tilde{D}(s) = n$, $\deg B(s) < \deg A(s) = m$, and then the degree of $F(s)$ is at most $n+m$.

S2b: Write the following:

$$
\begin{aligned}
A(s) &= A_0 + A_1 s + A_2 s^2 + \cdots + A_m s^m \\
B(s) &= B_0 + B_1 s + B_2 s^2 + \cdots + B_m s^m \\
N_p(s) &= N_0 + N_1 s + N_2 s^2 + \cdots + N_n s^n \\
\tilde{D}(s) = D_p(s)\phi(s) &= \tilde{D}_0 + \tilde{D}_1 s + \tilde{D}_2 s^2 + \cdots + \tilde{D}_n s^n \\
F(s) &= F_0 + F_1 s + F_2 s^2 + \cdots + F_{n+m} s^{n+m},
\end{aligned}
$$

where all coefficients are real constants, some of which are zero.

S2c: Match all the like powers of s of equation (4.5) and then solve for the coefficients of $A(s)$ and $B(s)$:

$$\begin{aligned} A_0\tilde{D}_0 + B_0N_0 &= F_0 \\ A_0\tilde{D}_1 + A_1\tilde{D}_1 + B_0N_1 + N_0B_1 &= F_1 \\ &\vdots \\ A_m\tilde{D}_n + B_mN_n &= F_{n+m}, \end{aligned}$$

or in the matrix form:

$$\begin{bmatrix} A_0 & B_0 & A_1 & B_1 & \cdots & A_m & B_m \end{bmatrix} \mathcal{S}_m = \begin{bmatrix} F_0 & F_1 & \cdots & F_{n+m} \end{bmatrix}, \tag{4.6}$$

where

$$\mathcal{S}_m = \begin{bmatrix} \tilde{D}_0 & \tilde{D}_1 & \dots & \tilde{D}_n & 0 & \dots & 0 \\ N_0 & N_1 & \dots & N_n & 0 & \dots & 0 \\ \dots & \dots & \dots & \dots & \dots & \dots & \dots \\ 0 & \tilde{D}_0 & \dots & \tilde{D}_{n-1} & \tilde{D}_n & \dots & 0 \\ 0 & N_0 & \dots & N_{n-1} & N_n & \dots & 0 \\ \dots & \dots & \dots & \dots & \dots & \dots & \dots \\ \vdots & \vdots & \vdots & \vdots & \vdots & \vdots & \vdots \\ \dots & \dots & \dots & \dots & \dots & \dots & \dots \\ 0 & 0 & \dots & 0 & \tilde{D}_0 & \dots & \tilde{D}_n \\ 0 & 0 & \dots & 0 & N_0 & \dots & N_n \end{bmatrix}.$$

4.2 Repetitive Control

We consider a general periodic disturbance $d(t)$ with a known period in the closed-loop system shown in Figure 4.3, where $D(s)$, $Y(s)$, $R(s)$ are respectively the Laplace transform of $d(t)$, $y(t)$, $r(t)$. The disturbance $D(s)$ with period τ_d is given by

$$D(s) = \mathcal{L}\left[d(t)\right] = \frac{1}{1 - e^{-\tau_d s}} \int_0^T e^{-st} d(t) dt.$$

In view of the internal model principle from the previous section, we expect that the closed-loop system in Figure 4.3 achieves asymptotic disturbance rejection with an appropriate

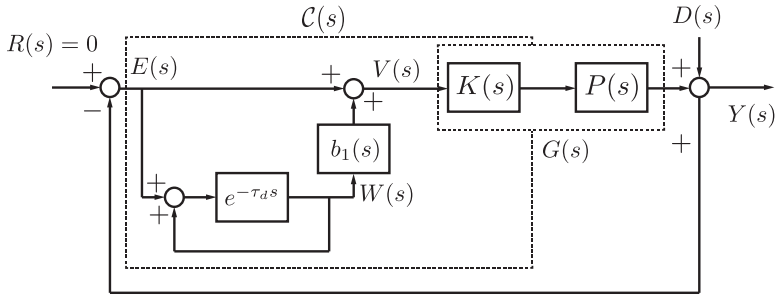

Figure 4.3: Closed-loop system with a repetitive controller.

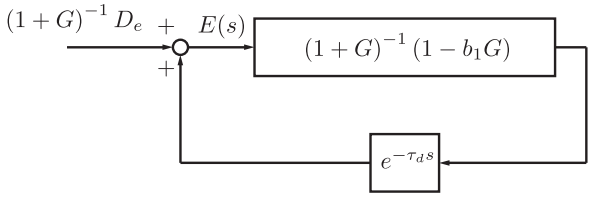

Figure 4.4: A system equivalent to Figure 4.3.

proper controller $K(s)$ and an internal model $\frac{1}{\phi(s)} = \frac{1}{1-e^{-\tau_d s}}$, which is called a repetitive controller. To see if the expectation holds, we study the stability of system below [9]. Note that we say a transfer function is stable or asymptotically stable if the poles of the transfer function have negative real parts.

Consider the single-input single-output (SISO) system in Figure 4.3 where $G(s) = K(s)P(s)$ is a compensated plant that is a strictly proper transfer function, $b_1(s)$ is a proper transfer function, and $Y(s)$, $D(s)$, and $E(s)$ are respectively the Laplace transform of the output $y(t)$, the bounded continuous periodic disturbance $d(t)$, and the error signal $e(t)$. The following relations from the SISO system hold:

$$E(s) = -Y(s) \tag{4.7}$$
$$Y(s) = G(s)V(s) + D(s) + \bar{Y}(s) \tag{4.8}$$
$$V(s) = E(s) + b_1(s)W(s) \tag{4.9}$$
$$W(s) = e^{-\tau_d s}\left[W(s) + E(s)\right] + \bar{W}(s), \tag{4.10}$$

where $\bar{Y}(s)$ and $\bar{W}(s)$ are respectively the initial responses of $G(s)$ and $e^{-\tau_d s}$. We use equations (4.7) to (4.10) to get

$$E(s) = e^{-\tau_d s}\left(1+G(s)\right)^{-1}\ \left(1 - b_1(s)G(s)\right)E(s) + \left(1+G(s)\right)^{-1}D_e(s), \tag{4.11}$$

where

$$D_e(s) = \left(1 - e^{-\tau_d s}\right)\left(-D(s) - \bar{Y}(s)\right) - G(s)\bar{W}(s). \tag{4.12}$$

Equation (4.11) is used to form the equivalent system shown in Figure 4.4. Bounded-input bounded-output (BIBO) stability of the equivalent system is guaranteed if the two conditions below are satisfied; see [9] or Appendix A.4 for proof.

1) $(1+G)^{-1}G$ is asymptotically stable,

2) the following inequality is satisfied:

$$\| (1+G)(1-b_1 G) \|_\infty < 1 \tag{4.13}$$

where $\| \cdot \|_\infty = \sup_\omega | \cdot |$.

In other words for any bounded continuous periodic disturbance of period τ_d, if both 1) and 2) are satisfied, then the error signal

$$e(t) = \mathcal{L}^{-1}[E(s)] \in \mathbf{L_2}, \tag{4.14}$$

where $e(t) \in \mathbf{L_2}$ if $\int_0^\infty e(t)e(t)dt < \infty$. We see that 2), however, cannot be satisfied for strictly proper transfer function $G(s)$, because $G(j\omega) \to 0$ as $\omega \to \infty$, and then $\| \cdot \|_\infty = 1$, which violates the inequality in equation (4.13). We can conclude that the equivalent system in Figure 4.4 is not BIBO stable. Therefore, the stability of the closed-loop system cannot be achieved with the internal model $\frac{1}{\phi(s)}$.

The failure of a repetitive controller in guaranteeing the closed-loop stability with strictly proper compensated plant $G(s)$ can be reasoned by Theorem 1 in Section 4.1. It states that asymptotic disturbance rejection is possible when the plant zeros do not cancel the poles of the disturbance. Applying this principle to the current situtation (although it is nonclassical), we see that it is not satisfied, because $G(s)$ has infinity as its zero whereas the periodic disturbance has a pole of arbitrary high frequency [9].

The demand in asymptotic disturbance rejection for any general periodic disturbance is apparently unrealistic, because the disturbance contains arbitrarily high frequency modes. Therefore, we expect the stability condition can be relaxed, at the expense of asymptotic disturbance rejection, by reducing the loopgain in the higher frequency range. This leads to the idea of replacing $e^{-\tau_d s}$ by $q_1(s)e^{-\tau_d s}$ for a suitable function $q_1(s)$, such that $|q_1(j\omega)| < 1$ for all ω. The controller of this type is called the modified repetitive controller.

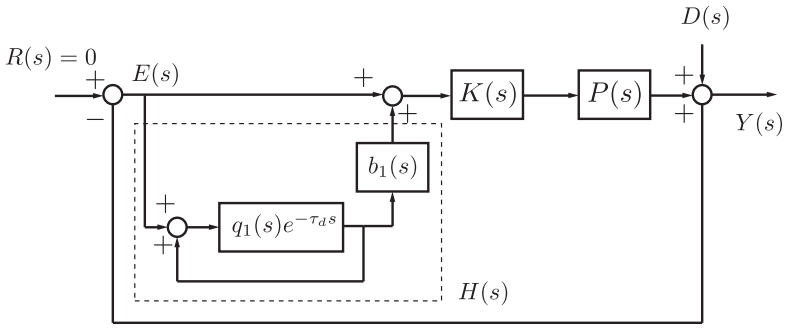

Figure 4.5: Closed-loop system with a modified repetitive controller.

4.3 Modified Repetitive Control

We study the stability condition and synthesis procedure for the closed-loop system in Figure 4.5 where $H(s)$ is called the modified repetitive controller. The stability of the system is given in the next theorem.

Theorem 2 ([9] or [10])**.** *Consider the closed-loop system shown in Figure 4.5 with a strictly proper plant $P(s)$, stable proper transfer functions $q_1(s)$ and $b_1(s)$, a proper transfer function $K(s)$, and bounded continuous periodic disturbance $d(t)$ with period τ_d. If*

C1a: *the transfer function $\frac{K(s)P(s)}{1+K(s)P(s)}$ is asymptotically stable,*

C2a: *the following inequality is satisfied:*

$$R(\omega) = |q_1(j\omega)F(j\omega)| < 1 \quad \forall \omega \geq 0, \tag{4.15}$$

where

$$F(j\omega) = 1 - b_1(j\omega)\frac{KP(j\omega)}{1 + KP(j\omega)}, \tag{4.16}$$

then the closed-loop system is asymptotically stable and the output $y(t)$ is bounded.

Proof. We compute the transfer function from $D(s)$ to $Y(s)$:

$$\begin{aligned} Y(s) &= D(s) - \left(1 + b_1(s)\frac{q_1(s)e^{-\tau_d s}}{1 - q_1(s)e^{-\tau_d s}}\right) K(s)P(s)Y(s) \\ &= \frac{\left(1 - q_1(s)e^{-\tau_d s}\right) D(s)}{1 + K(s)P(s) + \left(b_1(s)K(s)P(s) - K(s)P(s) - 1\right) q_1(s)e^{-\tau_d s}}. \end{aligned}$$

The poles of the transfer function is given as

$$1 + K(s)P(s) + (b_1(s)K(s)P(s) - K(s)P(s) - 1)\, q_1(s)e^{-\tau_d s}. \tag{4.17}$$

Let the following

$$P(s) = \frac{N_p(s)}{D_p(s)}, \qquad K(s) = \frac{B(s)}{A(s)}, \qquad b_1(s) = \frac{N_b(s)}{D_b(s)}, \qquad q_1(s) = \frac{N_q(s)}{D_q(s)},$$

then the poles (4.17) can be written as

$$D_b D_q\,(AD_p + BN_p) + [N_q N_b B N_p - D_b N_q\,(AD_p + BN_p)]\, e^{-\tau_d s}.$$

We apply Theorem 4 in Appendix A.5 with $X(s) = D_b D_q\,(AD_p + BN_p)$, where $\deg X = n$ and $Z(s) = [N_q N_b B N_p - D_b N_q\,(AD_p + BN_p)]$, where $\deg Z = m < n$ since $q_1(s)$ and $P(s)$ are strictly proper. The condition that $|b_{n1}| < 1$ is satisfied since $\deg Z < \deg X$; the condition that all the roots of $D_b D_q\,(AD_p + BN_p)$ have negative real parts implies $\frac{K(s)P(s)}{1+K(s)P(s)}$ is asymptotically stable since $q_1(s)$ and $b_1(s)$ are stable. The condition that $\left|\frac{Z(j\omega)}{X(j\omega)}\right| < 1$ $\forall\omega \geq 0$ implies condition **C2a** since $|e^{-j\omega\tau_d}| = 1$. Therefore, the closed-loop system is asymptotically stable. The output $y(t)$ is bounded, since $\mathcal{L}^{-1}\left[(1 - q_1(s)e^{-\tau_d s})D(s)\right]$ is bounded.

□

4.3.1 Synthesis Procedure

Condition **C1a** is equivalent to constructing a controller $K(s)$ so that the closed-loop system is asymptotically stable when $H(s) = 0$. One method to construct $K(s)$ is to carry out the pole-placement in the same way as **S2** in Section 4.1. Another method, which is explained here, is to use an observer-based feedback controller. This type of feedback controller has the advantage that the controllable but unobservable poles can be reassigned [16]. Given a realization (A, B, C) of $P(s)$ in Figure 4.5 that is stabilizable and detectable, the observer-based feedback controller is given as:

$$\dot{\hat{x}}(t) = A\hat{x}(t) + Bu(t) + L\,(y - C\hat{x}(t))\,, \tag{4.18}$$

$$u(t) = -G\hat{x}(t), \tag{4.19}$$

where the gain matrices G and L are to be designed. Since (A, B) is stabilizable and (C, A) is detectable, we can find gains G and L such that $A - BG$ and $A - LC$ are Hurtwitz [16].

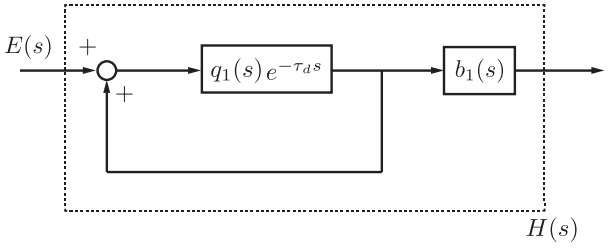

Figure 4.6: Modified repetitive controller.

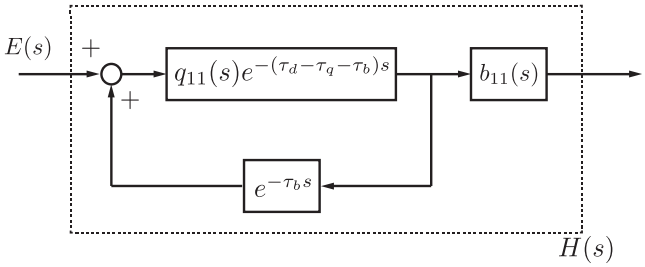

Figure 4.7: Implementable modified repetitive controller.

A way to compute such gains is to solve the algebraic Ricatti equations (ARE):

$$0 = A^T P + PA + Q - PBR^{-1}B^T P, \tag{4.20}$$

$$0 = AS + SA^T + V_1 - SC^T V_2^{-1} CS. \tag{4.21}$$

We choose (Q, A) to be detectable and (A, V_1) to be stabilizable to obtain unique solutions of P and Q in the ARE [20], and set

$$G = R^{-1}B^T P, \tag{4.22}$$

$$L = SC^T V_2^{-1}. \tag{4.23}$$

Furthermore, the controller $K(s)$ in Figure 4.5 is computed using the equation

$$K(s) = G\left(sI - A + BG + LC\right)^{-1} L. \tag{4.24}$$

Condition **C2a** is analyzed in the frequency domain to see the roles of $q_1(s)$ and $b(s)$. We see that $P(j\omega) \to 0$ as $\omega \to \infty$, because $P(s)$ is strictly proper so equation (4.15) implies that $R(\omega) \approx |q_1(j\omega)|$ for high frequencies. If $|q_1(j\omega)|$ is close to zero then stability is guaranteed but the disturbance rejection performance deteriorates because we expect

asymptotic disturbance rejection when $q_1(s) = 1$ from the internal model principle. Therefore, the design of $q_1(s)$ can be viewed as a trade-off between stability and performance [9]. In low frequency range, we see that if $b_1(j\omega) \approx \frac{1+KP(j\omega)}{KP(j\omega)}$ then $R(\omega) \approx 0$, which improves the stability of the system [10]. A proper transfer function is chosen for $|b_1(j\omega)|$ such that $|b_1(j\omega)| \approx \left|\frac{1+KP(j\omega)}{KP(j\omega)}\right|$ for low frequencies. It is customary to add small time advances to both $b_1(s)$ and $q_1(s)$ [13], and then define them as follows:

$$b_1(s) = b_{11}(s)e^{\tau_b s}, \qquad q_1(s) = q_{11}(s)e^{\tau_q s}, \qquad \tau_q, \tau_b > 0, \tag{4.25}$$

where $b_{11}(s)$ and $q_{11}(s)$ are proper transfer functions which are often low pass filters of first order or second order; τ_q and τ_b are chosen to be much smaller than τ_d, the period of the disturbance. The stability conditions of Theorem 2 remain the same, but an implementation problem occurs since τ_q and τ_b are positive. We can resolve this by absorbing τ_q and τ_b into τ_d. In other words, we transform the modified repetitive controller in Figure 4.6 into the one in Figure 4.7.

To summarize the design procedure discussed above, we give a detailed procedure.

T1: Find controller $K(s)$.

T1a: Choose Q, R, V_1 and V_2 such that (Q, A) is detectable, (A, V_1) is stabilizable, and other desired closed-loop characteristics are met.

T1b: Solve the algebraic Riccati equations (4.20) and (4.21) for unique P and S, and then use equations (4.22) and (4.23) for gains G and L.

T1c: Use equation (4.24) to compute $K(s)$.

T2: Find $b_1(s)$ and then $q_1(s)$.

T2a: Use a Bode plot of $\frac{1+KP(j\omega)}{KP(j\omega)}$ and change parameters in $b_{11}(s)$ such that they are approximately equal up to a certain frequency, ω_b.

T2b: Choose τ_b, which is much less than τ_d, so that e^{τ_b} cancels the negative phase of $\frac{KP(s)}{1+KP(s)}$ up to ω_b.

T2c: Choose parameters in $q_{11}(s)$ such that the inequality (4.15) is satisfied. The cutoff frequency of $q_{11}(s)$ should be greater than ω_b in step **T2a**.

T2d: Choose τ_q, which is much less than τ_d, so that e^{τ_q} cancels the negative phase of $q_{11}(s)$ up to its cutoff frequency.

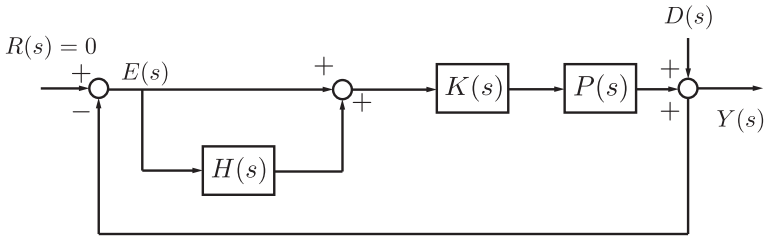

Figure 4.8: Closed-loop system with a two-period modified repetitive controller.

We note that if the design specifications involve requirements on the sensitivity function, then a procedure already exists; see [13].

4.4 Two Period Modified Repetitive Control

We study the stability condition and synthesis procedure of the closed-loop system in Figure 4.8 with a disturbance $d(t)$ that is a sum of two periodic functions with known periods, τ_{d_1} and τ_{d_2}, that are irrationally related, i.e., τ_{d_1}/τ_{d_2} is an irrational number. If the periods are rationally related then the one period modified repetitive controller in the previous section can be tuned to the least common multiple of the two periods. For irrationally related periods, a new configuration for the modified repetitive controller is needed, which we call the two period modified repetitive controller.

The two period modified repetitive controller suggested in [14] is given as follows:

$$H(s) = b_1(s)\left[\frac{q_1(s)e^{-\tau_{d_1}s}}{1-q_1(s)e^{-\tau_{d_1}s}} + \frac{q_2(s)e^{-\tau_{d_2}s}}{1-q_2(s)e^{-\tau_{d_2}s}} + \frac{q_1(s)q_2(s)e^{-(\tau_{d_1}+\tau_{d_2})s}}{(1-q_1(s)e^{-\tau_{d_1}s})\,(1-q_2(s)e^{-\tau_{d_2}s})}\right], \tag{4.26}$$

where $b_1(s)$, $q_1(s)$, and $q_2(s)$ are to be designed. The stability of the closed-system with $H(s)$ in equation (4.26) is given in the next theorem.

Theorem 3 ([14]). *Consider the closed-loop system in Figure 4.8 with a strictly proper plant $P(s)$, $H(s)$ in equation (4.26), stable proper transfer functions $q_1(s)$, $q_2(s)$, $b_1(s)$, and $K(s)$. The bounded continuous disturbance $d(t)$ is given as the sum of two periodic functions with known periods, τ_{d_1} and τ_{d_2}, that are irrationally related. If*

C1b: *the transfer function $\frac{K(s)P(s)}{1+K(s)P(s)}$ is asymptotically stable,*

C2b: *the following inequality is satisfied:*

$$M(\omega) = |F(j\omega)| \left(|q_1(j\omega)| + |q_2(j\omega)| + |q_1 q_2(j\omega)|\right) < 1 \quad \forall \omega \geq 0, \tag{4.27}$$

where $F(j\omega)$ is given in equation (4.16),

then the closed-loop system is asymptotically stable and the output $y(t)$ is bounded.

Proof. We compute the transfer function from $D(s)$ to $Y(s)$:

$$1 + KP + (b_1 KP - KP - 1)\left(q_1 e^{-\tau_{d_1} s} + q_2 e^{-\tau_{d_2} s} - q_1 q_2 e^{-\left(\tau_{d_1} + \tau_{d_2}\right) s}\right), \tag{4.28}$$

and then apply Theorem 4 in Appendix A.5 to this equation to obtain the two stability conditions. The first condition in Theorem 4 requires $\frac{K(s)P(s)}{1+K(s)P(s)}$ to be asymptotically stable. The second condition requires the inequality in (4.27) since $\left|e^{-j\omega\tau_{d_1}}\right| = \left|e^{-j\omega\tau_{d_2}}\right| = 1$. Therefore, the closed-loop system is asymptotically stable. The output $y(t)$ is bounded, since $\mathcal{L}^{-1}\left[\left(1 - q_1 e^{-\tau_{d_1} s}\right)\left(1 - q_2 e^{-\tau_{d_2} s}\right) D(s)\right]$ is bounded. □

4.4.1 Synthesis Procedure

The design of the stabilizing controller $K(s)$ in Condition **C1b** is equivalent to Condition **C1a**. In Condition **C2b**, we propose that each repetitive controller is designed one at a time; that is, find $q_1(s)$ and $b_1(s)$ satisfying **C2a**, and then find $q_2(s)$ satisfying **C2b**. If we assume $q_1(s)$ and $b_1(s)$ are known, then we solve the inequality (4.27) for $|q_2(j\omega)|$:

$$|q_2(j\omega)| < \frac{1 - |F(j\omega)|\,|q_{11}(j\omega)|}{|F(j\omega)|\,(1 + |q_{11}(j\omega)|)} =: N(j\omega). \tag{4.29}$$

We add small time advances to the filters $b_1(s)$, $q_1(s)$, and $q_2(s)$, and then define them as follows:

$$b_1(s) = b_{11}(s)e^{\tau_b s}, \quad q_1(s) = q_{11}(s)e^{\tau_{q_1} s}, \quad q_2(s) = q_{22}(s)e^{\tau_{q_2} s}, \quad \tau_{q_1}, \tau_{q_2}, \tau_b > 0, \tag{4.30}$$

where $b_{11}(s)$, $q_{11}(s)$, $q_{22}(s)$ are transfer functions which are often low pass filters of first order or second order; τ_b, τ_{q_1}, and τ_{q_2} are chosen to be much smaller than τ_{d_1} or τ_{d_2}. With these newly defined transfer functions, the stability conditions of Theorem 3 remain the same, but an implementation problem can arise, because τ_b, τ_{q_1}, and τ_{q_2} are positive. To resolve the issue, we transform the two period modified repetitive controller in Figure 4.9 into the one in Figure 4.10.

The design procedure discussed is summarized in detail here.

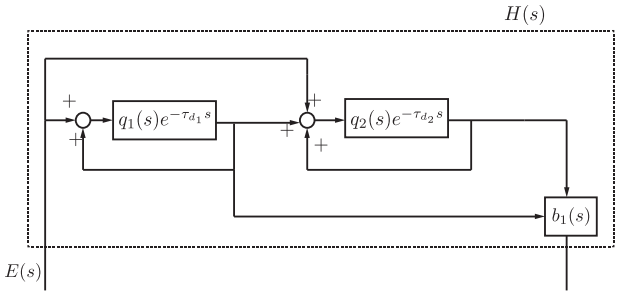

Figure 4.9: Two period modified repetitive controller.

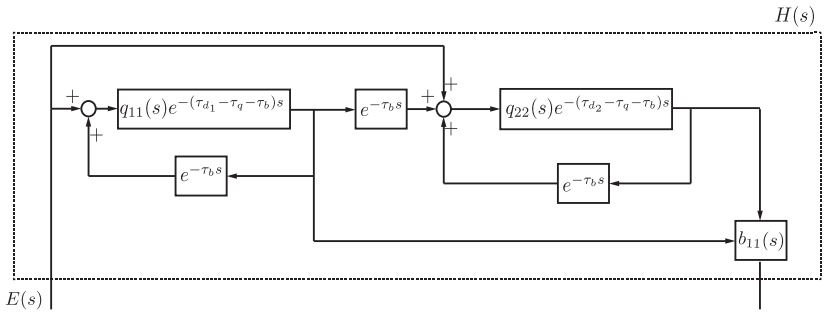

Figure 4.10: Implementable two period modified repetitive controller.

U1: Find $K(s)$, $b_1(s)$ and $q_1(s)$ using the procedure in the last section.

U2: Find $q_2(s)$.

U2a: If $q_{22}(s)$ is of first order

$$q_{22}(s) = \frac{1}{a_1 s + 1}, \tag{4.31}$$

then equation (4.29) becomes

$$\left[\omega^2 a_1^2 + 1\right] N^2(j\omega) - 1 > 0 \quad \forall \omega \geq 0. \tag{4.32}$$

U2b: If $q_{22}(s)$ is of second order

$$q_{22}(s) = \frac{a_2}{s^2 + a_3 s + a_2}, \tag{4.33}$$

then equation (4.29) becomes

$$\left[N^2(j\omega) - 1\right] a_2^2 + \left[\omega^2 N^2(j\omega)\right] a_3^2 + \left[-2\omega^2 N^2(j\omega)\right] a_2 + \omega^4 N^2(j\omega) \geq 0 \quad \forall \omega > 0. \tag{4.34}$$

U3b: We choose τ_{q_2}, which is much less than τ_d, so that $e^{\tau_{q_2}}$ cancels the negative phase of $q_{22}(s)$ up to its cutoff frequency.

If a_1 satisfies the inequality (4.32) for all frequencies $\omega \geq 0$, or if a_2, a_3 satisfies the inequality (4.34) for all frequencies $\omega \geq 0$, then condition **C2b** is satisfied. There is a possibility for certain transfer functions $b_1(s)$, $q_1(s)$, or $K(s)$ that no solutions of a_1 or a_2, a_3 in $q_{22}(s)$ exist. The nonexistence of a solution may be due to the restrictiveness of the transfer functions. For example, if we designed $b_1(s)$, $q_1(s)$, and $K(s)$ so that $R(\omega)$ is slightly less than 1 for some ω, then the condition $M(\omega) < 1$ will likely not be satisfied, since $M(\omega)$ is essentially $R(\omega)$ plus other terms. In this case, the user must then redesign $K(s)$ by choosing different gains G and L or choose different parameters in $b_1(s)$ and $q_1(s)$.

Chapter 5

Application

In this chapter, the internal model principle and the repetitive control strategy are applied to reduce the effect of disturbances on the lateral motion of the five-roller web system.

We take the Laplace transform of the state-space equations (2.35) with $w(t) = y_0(t)$:

$$\begin{aligned} X(s) &= (sI - A)^{-1}BU(s) + (sI - A)^{-1}FY_0(s) \\ Y(s) &= C(sI - A)^{-1}BU(s) + C(sI - A)^{-1}FY_0(s), \end{aligned} \tag{5.1}$$

where $U(s)$, $Y_0(s)$ are respectively the Laplace transform of $u(t)$, $y_0(t)$. Using equation (5.1), we get the closed-loop system in Figure 5.1. The plant transfer function $P(s)$ is

$$P(s) = C(sI - A)^{-1}B = \frac{1}{s^2}, \tag{5.2}$$

and the disturbance $G_d(s)Y_0(s)$ is

$$\begin{aligned} G_d(s)Y_0(s) &= C(sI - A)^{-1}FY_0(s) \\ &= \frac{1.1s^2 - 1.2s + 45.7}{s^4 + 7.5s^3 + 27.7s^2 + 50.6s + 45.7}Y_0(s). \end{aligned}$$

Three simulations studies are conducted on this system. In Section 5.1, an internal model controller is synthesized for a sinusoidal disturbance $y_0(t)$. In Section 5.2, a modified repetitive controller is synthesized for a general periodic disturbance. In Section 5.3, a two period modified repetitive controller is synthesized for a disturbance that is the sum of two periodic functions.

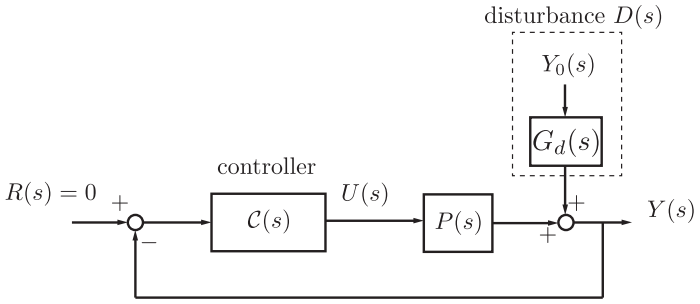

Figure 5.1: Closed-loop of the five-roller web system.

5.1 Simulation Results for Internal Model Principle

Consider the closed-loop system shown in Figure 5.2. Our objective is to synthesize $B(s)$, $A(s)$, and $\phi(s)$ so that the closed-loop system asymptotically rejects a sinusoidal disturbance. The procedure in Section 4.1 is used here. The disturbance has amplitude $\alpha = 3.81$mm and known period $\frac{2\pi}{0.2}$s:

$$y_0(t) = \alpha \sin(0.2t),$$
$$\mathcal{L}[y_0(t)] = Y_0(s) = \frac{\alpha}{s^2 + 0.04}.$$

The internal model contains the unstable poles of the disturbance $G_d(s)Y_0(s)$, so $\phi(s) = s^2 + 0.04$, because all the poles of $G_d(s)$ are stable.

Next, we carry out the pole placement problem for $F(s)$. Since $\tilde{D}(s) = D_p(s)\phi(s)$ is degree 4, choose $B(s)$ and $A(s)$ to be of degree 3. As a result, $F(s)$ is at most degree 7:

$$\begin{aligned} F(s) &= A(s)\tilde{D}(s) + B(s)N_p(s) \\ &= \left(A_0 + A_1 s + A_2 s^2 + A_3 s^3\right)\left(s^2 + 0.04\right) s^2 + B_0 + B_1 s + B_2 s^2 + B_3 s^3. \end{aligned} \tag{5.3}$$

If the desired roots of the polynomial $F(s)$ is

$$F(s) = (s+2)\left(s^2 + 4s + 5\right)\left(s^2 + 2s + 5\right)\left(s^2 + 6s + 10\right), \tag{5.4}$$

then the coefficients A_i and B_i, $i = 1, 2, 3$ can be solved using procedure **S2** from Section 4.1. The controller is

$$K(s) = \frac{B(s)}{A(s)} = \frac{778s^3 + 1207s^2 + 1150s + 500}{s^3 + 14s^2 + 88s + 325}.$$

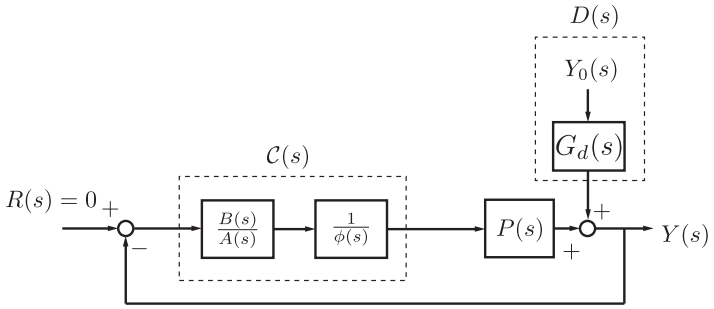

Figure 5.2: Closed-loop system with internal model.

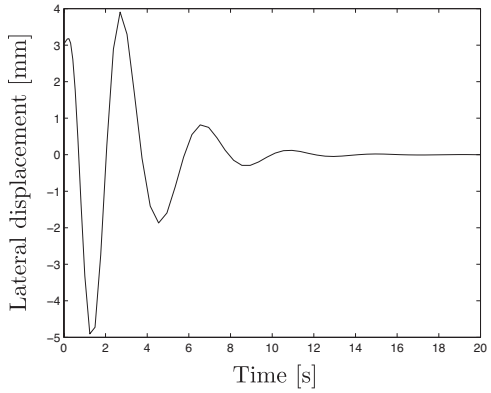

Figure 5.3: Internal model: output $y_2(t)$.

The simulation result for some nonzero initial condition is shown in Figure 5.3. We see that asymptotic disturbance rejection is achieved; that is, the output $y_2(t)$, lateral displacement of the web at roller R_2, converges to zero even in the presence of a sinusoidal disturbance $y_0(t)$.

5.2 Simulation Results for Modified Repetitive Control

Consider the closed-loop system shown in Figure 5.4. Our objective is to synthesize a modified repetitive controller $H(s)$, and a stabilizing controller $K(s)$, so that the closed-loop system rejects a periodic disturbance $y_0(t)$. In the simulation study, we use triangular and sinusoidal disturbances with procedure in Section 4.3.

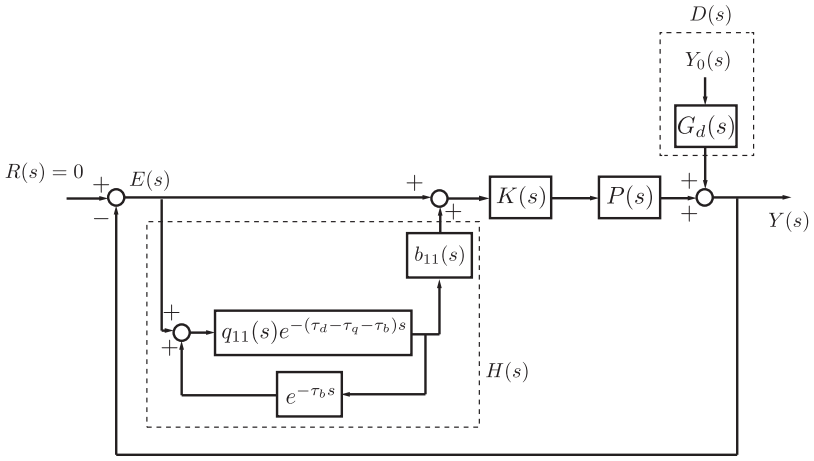

Figure 5.4: Closed-loop system with a modified repetitive controller.

5.2.1 Sinusoidal Disturbances

The disturbance $y_0(t)$ is a sinusoidal function with amplitude $\alpha = 3.81$mm and period 10π:

$$y_0(t) = \alpha \sin(0.2t).$$

We start the procedure by synthesizing $K(s)$ in **C1a** of Theorem 2. The values of R, V_2, Q, and V_1 are chosen in a way that (Q, A) is detectable and (A, V_1) is stabilizable: $R = V_2 = 1$,

$$Q = \text{diag}\begin{bmatrix} 0 & 0 & 1000 & 400 & 1000 & 400 & 1000 & 400 & 0 & 0 \end{bmatrix},$$

$$V_1 = \begin{bmatrix} 0 & 0 & 0 & 0 & 0 & 0 & 0 & 0 & 0 & 0 \\ 0 & 0 & 0 & 0 & 0 & 0 & 0 & 0 & 0 & 0 \\ 0 & 0 & 0 & 0 & 0 & 0 & 0 & 0 & 0 & 0 \\ 0 & 0 & 0 & 5000 & 0 & 0 & 0 & 0 & 0 & 5000 \\ 0 & 0 & 0 & 0 & 0 & 0 & 0 & 0 & 0 & 0 \\ 0 & 0 & 0 & 0 & 0 & 0 & 0 & 0 & 0 & 0 \\ 0 & 0 & 0 & 0 & 0 & 0 & 0 & 0 & 0 & 0 \\ 0 & 0 & 0 & 0 & 0 & 0 & 0 & 0 & 0 & 0 \\ 0 & 0 & 0 & 0 & 0 & 0 & 0 & 0 & 0 & 0 \\ 0 & 0 & 0 & 5000 & 0 & 0 & 0 & 0 & 0 & 5000 \end{bmatrix}.$$

The AREs are solved for P and S and then we use the gain equations (4.22) and (4.23) to

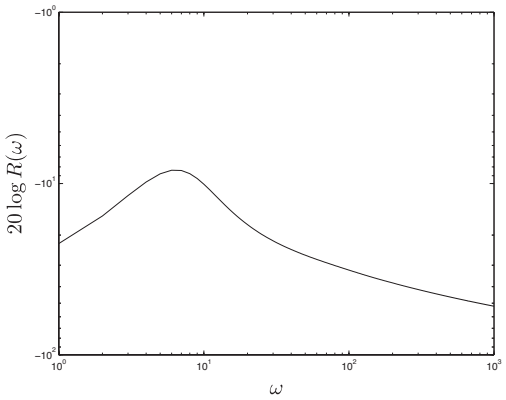

Figure 5.5: $R(\omega)$ in Condition **C2a**.

compute G and L:

$$G = \begin{bmatrix} 6.2 & -4.7 & 106.8 & 15.3 & 30.8 & 9.3 & 24.5 & 13.0 & 8.5 & 9.8 \end{bmatrix},$$
$$L = \begin{bmatrix} 0 & 0 & 11.9 & 70.7 & 0.1 & 3.2 & 0.1 & 2.3 & 11.9 & 70.7 \end{bmatrix}^T.$$

The stabilizing controller $K(s)$ can be computed using equation (4.24):

$$K(s) = \frac{3211s^5 + 24000s^4 + 79800s^3 + 147000s^2 + 146500s + 72100}{s^6 + 41.7s^5 + 669.5s^4 + 2686s^3 + 5579s^2 + 5875s + 2939}. \tag{5.5}$$

Next, we find the transfer functions $b_1(s)$ and $q_1(s)$ to satisfy **C2a** of Theorem 2. Choose $b_{11}(s) = 1$ since $\frac{KP(j\omega)}{1+KP(j\omega)}$ has a magnitude close to 0 from $\omega = 0$ to $\omega = 2.5$. Pick $\tau_b = 0.07$, because the phase of $e^{0.07s}$ approximately cancels the phase of $\frac{KP(j\omega)}{1+KP(j\omega)}$ in the same frequency range. Choose $q_{11}(s)$ that satisfies condition **C2a** (i.e., the inequality $R(\omega) < 1$ in equation (4.15)):

$$q_{11}(s) = \frac{1}{0.4s + 1};$$

see Figure 5.5 for a plot of $R(\omega)$ from $\omega = 0$ to $\omega = 10^3$. Pick $\tau_{q_1} = 0.4$ since the phase of $e^{0.4s}$ approximately cancels the phase of $q_{11}(s)$ below its cut-off frequency.

A comparison of the disturbance rejection performance with and without the modified repetitive controller is demonstrated by turning on repetitive control at $t = 120$s. The simulation result for some nonzero initial condition is shown in Figure 5.6. We see that the steady-state lateral displacement at roller R_2 is reduced from 6.5 μm to 0.02 μm, a reduction of 99.7% in the presence of a modified repetitive controller. We see that the

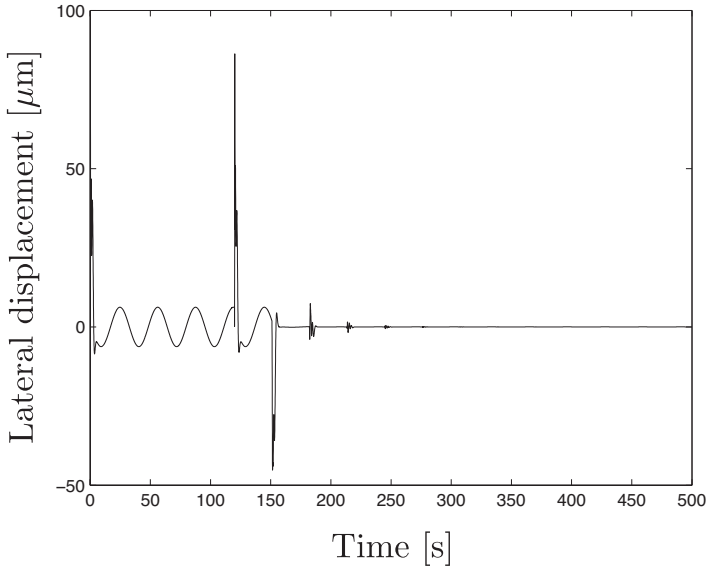

Figure 5.6: Simulation study: output, $y_2(t)$.

choice of filters $b_1(s)$ and $q_1(s)$ are not necessarily optimal for performance, but serves as a good demonstration of the effectiveness of the repetitive control strategy in rejecting the periodic disturbance.

5.2.2 Triangular Disturbance

The disturbance $y_0(t)$ is a triangular wave with amplitude $\alpha = 3.81$mm and period $\tau_d = 10\pi$; see Figure 5.7 for the disturbance. The Fourier series expansion of $y_0(t)$ is given by

$$y_0(t) = \frac{-8\alpha}{\pi^2} \sum_{n=0}^{\infty} \frac{1}{(2n+1)^2} \cos\left[(2n+1)\,\frac{2\pi}{\tau_d} t\right],$$

and the spectrum of this series is shown in Figure 5.8.

Using the same transfer functions $K(s)$, $b_1(s)$, and $q_1(s)$ in the previous subsection, a comparison of the disturbance rejection performance with and without the modified repetitive controller is demonstrated by turning on repetitive control at $t = 120$s. The simulation result for some nonzero initial condition is shown in Figure 5.9. The steady-state lateral displacement at roller R_2 is reduced from 36 μm to 5.5 μm, a reduction of 85% in the presence of a modified repetitive controller. We see that even in the case of a

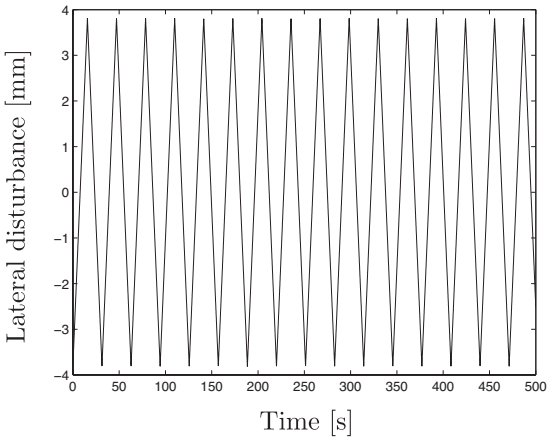

Figure 5.7: Triangle wave disturbance.

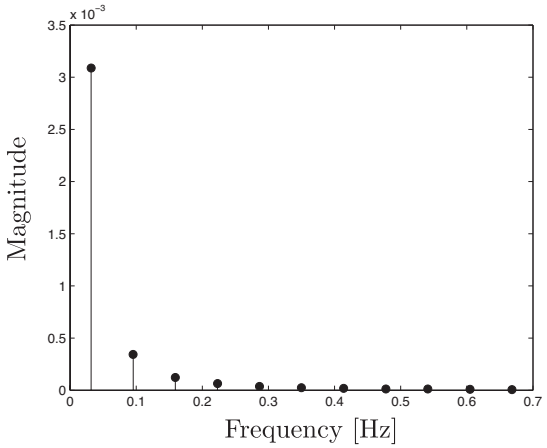

Figure 5.8: Spectrum of the triangular wave.

triangular disturbance, which is more problematic than a sinusoidal type, the disturbance rejection performance is still impressive.

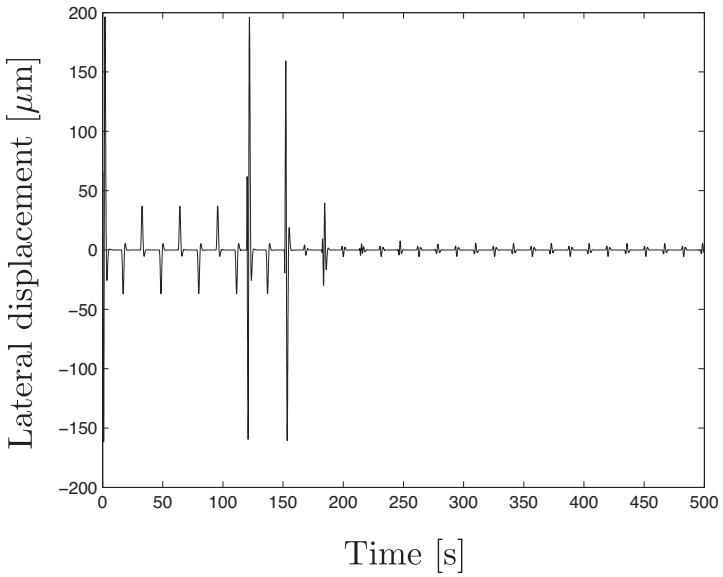

Figure 5.9: Simulation study: output, $y_2(t)$.

5.3 Simulation Results for Two Period Modified Repetitive Control

Consider the closed-loop system shown in Figure 5.10. Our objective is to synthesize a two period modified repetitive controller $H(s)$ and a stabilizing controller $K(s)$ so that the closed-loop system rejects a disturbance containing two periodic functions with irrationally related periods. In the simulation study, we use triangular and sinusoidal disturbances with procedure in Section 4.4.

5.3.1 Two Sinusoidal Disturbances

The disturbance $y_0(t)$ is the sum of two sinusoidal functions with amplitudes $\alpha_1 = 3.81$mm, $\alpha_2 = 3.81$mm and periods $\tau_{d_1} = \frac{2\pi}{\sqrt{0.1}}$s, $\tau_{d_2} = \frac{2\pi}{\sqrt{0.2}}$s; the disturbance is shown in Figure 5.11 and the spectrum is shown in Figure 5.12.

$$y_0(t) = \alpha_1 \sin(\sqrt{0.1}t) + \alpha_2 \sin(\sqrt{0.2}t)$$

The stabilizing controller $K(s)$ in equation (5.5) satisfies **C1b** of Theorem 3.

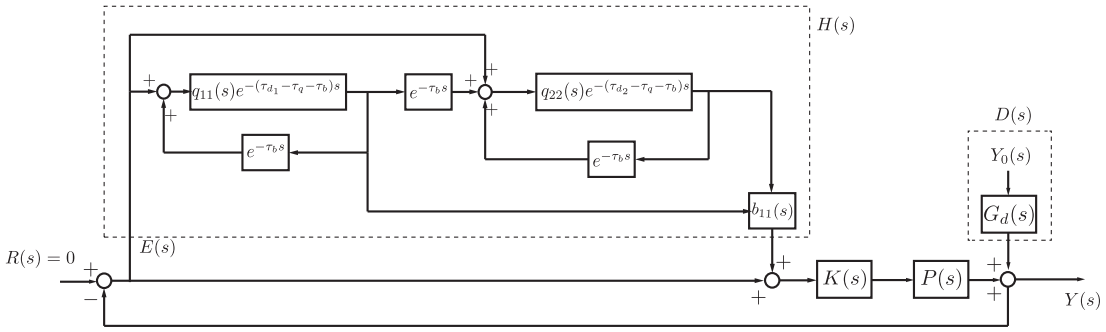

Figure 5.10: Closed-loop system with a two period modified repetitive controller.

Next, we find transfer functions $b_1(s)$, $q_1(s)$, and $q_2(s)$ to satisfy **C2b** of Theorem 3. The transfer functions $b_1(s)$ and $q_1(s)$ from Section 5.2 is used here:

$$b_1(s) = e^{0.07}, \qquad q_1(s) = \frac{1}{0.4s+1}e^{0.4s}.$$

The design of $q_2(s)$ involves finding $q_{22}(s)$ and τ_{q_2}. If $q_{22}(s)$ is of first order as in equation (4.31), then we compute the condition on a_1 for frequencies from $\omega = 0$ to $\omega = 10^3$. The choice of $a_1 = 0.4$ yields

$$q_{22}(s) = \frac{1}{0.4s+1},$$

which satisfies $M(\omega) < 1$; see Figure 5.13. If $q_{22}(s)$ is of second order as in equation (4.33), then we compute the condition on a_2 and a_3 for frequencies from $\omega = 0$ to $\omega = 10^3$. The choice of $a_2 = 3$ and $a_3 = 1$ yields

$$q_{22}(s) = \frac{3}{s^2+s+3},$$

which satisfies $M(\omega) < 1$; see Figure 5.13. Pick $\tau_{q_2} = 0.4$, because the phase of $e^{0.4s}$ approximately cancels the phase of $q_{22}(s)$ below its cut-off frequency.

A comparison of the disturbance rejection performance with and without the two period modified repetitive controller is demonstrated by turning on repetitive control at $t = 120$s. The simulation result with the first-order filter $q_{22}(s)$ is shown Figure 5.14, and the result for the second-order filter $q_{22}(s)$ is shown Figure 5.15. In the case of the first-order $q_{22}(s)$, we see that the steady-state lateral displacement is reduced from 48.8 μm to 1.2 μm, a reduction of 97.5%. In the case of the second-order $q_{22}(s)$, we observe that the steady-state lateral displacement is reduced from 48.8 μm to 4.0 μm, a reduction of 91.8%. The disturbance rejection performance of the first-order filter is superior to that of second-order filter, which is consistent with the simulation study for an optical disk drive [11].

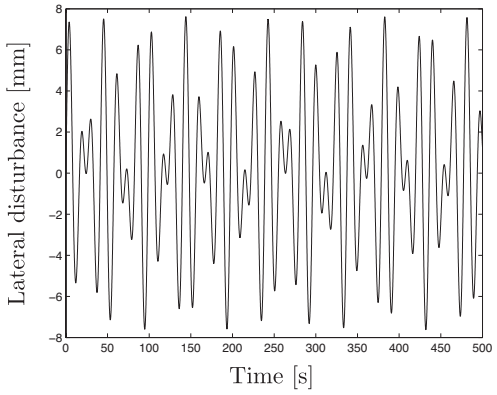

Figure 5.11: Sum of two sinusoidal waves

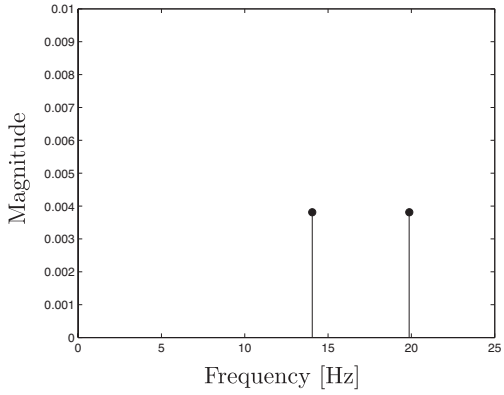

Figure 5.12: Spectrum of disturbance

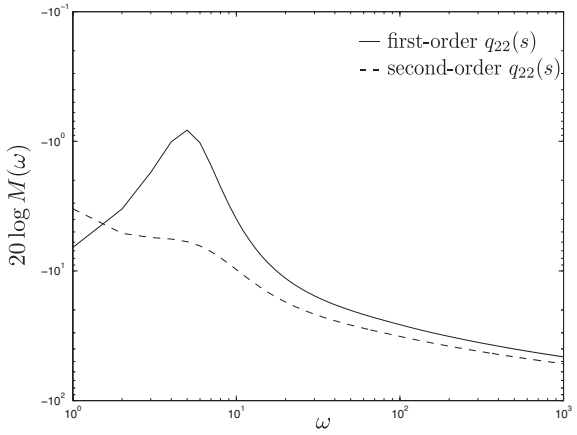

Figure 5.13: $M(\omega)$ in Condition **C2b**.

5.3.2 Two Triangular Disturbances

The disturbance $y_0(t)$ is the sum of two triangular waves with amplitudes $\alpha_1 = 3.81$mm, $\alpha_2 = 3.81$mm, and periods $\tau_{d_1} = \frac{2\pi}{\sqrt{0.1}}$s, $\tau_{d_2} = \frac{2\pi}{\sqrt{0.2}}$s; see Figure 5.16 for the disturbance. The Fourier series expansion of $y_0(t)$ is given by

$$y_0(t) = \frac{-8\alpha_1}{\pi^2} \sum_{n=0}^{\infty} \frac{1}{(2n+1)^2} \cos\left[(2n+1)\frac{2\pi}{\tau_{d_1}} t\right] + \frac{-8\alpha_2}{\pi^2} \sum_{n=0}^{\infty} \frac{1}{(2n+1)^2} \cos\left[(2n+1)\frac{2\pi}{\tau_{d_2}} t\right],$$

and the spectrum of the series is shown in Figure 5.17.

Using the same transfer functions $K(s)$, $b_1(s)$, $q_1(s)$, and $q_2(s)$ from the previous sub-

section, a comparison of the disturbance rejection performance with and without the two period modified repetitive controller is demonstrated by turning on repetitive control at $t = 120$s. The simulation result with the first-order filter $q_{22}(s)$ is shown Figure 5.18. We see that the steady-state lateral displacement is reduced from 82.6 μm to 13.3 μm, a reduction of 84%.

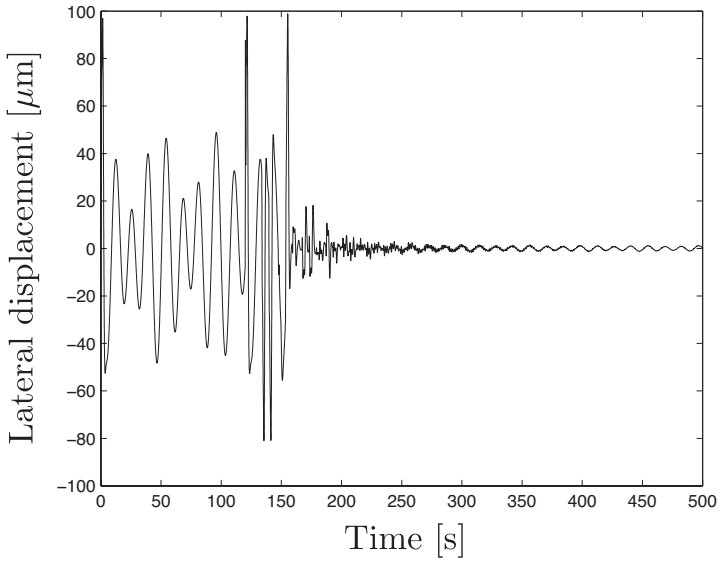

Figure 5.14: First-order low pass filter $q_{22}(s)$: output $y_2(t)$.

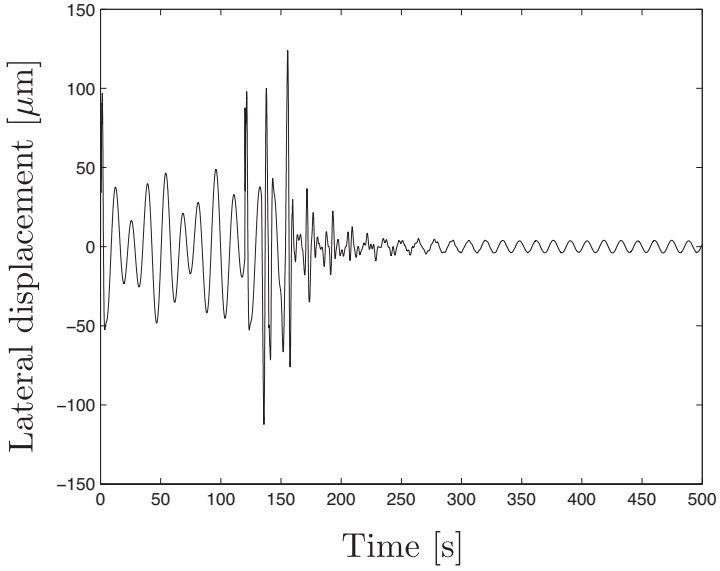

Figure 5.15: Second-order low pass filter $q_{22}(s)$: output $y_2(t)$.

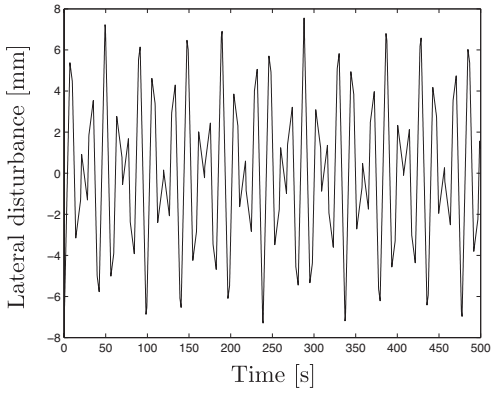

Figure 5.16: Sum of two triangular waves.

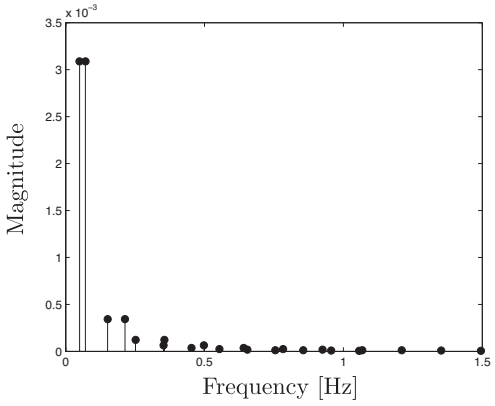

Figure 5.17: Spectrum of the disturbance.

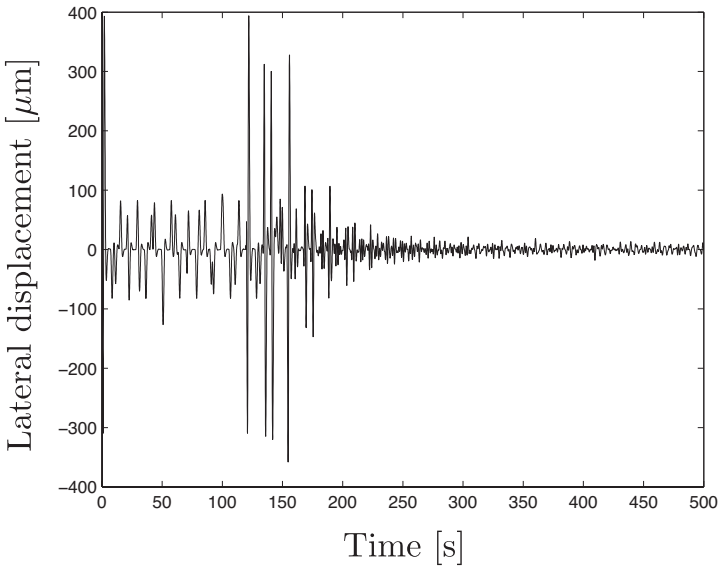

Figure 5.18: First-order low pass filter $q_{22}(s)$: output, $y_2(t)$.

Chapter 6

Conclusions

In this thesis, we have provided synthesis procedures for the control strategies of the internal model principle and repetitive control. By using these procedures, we have successfully synthesized an internal model controller, a modified repetitive controller, and a two period modified repetitive controller to reject disturbances from the lateral displacement in a roll-to-roll web system. The effectiveness of the controllers are demonstrated by several simulation studies on a five-roller web system. The results show that: 1) if the system contains an internal model controller and is under the influence of a sinusoidal disturbance, then the system achieves asymptotic disturbance rejection; 2) if the system contains a modified repetitive controller and is under the influence of a periodic disturbance, either sinusoidal or triangular, then we see a significant improvement in disturbance rejection compared with observer-based feedback control; 3) if the system contains a two period modified repetitive controller and is under the influence of a disturbance that is the sum of two periodic functions, then we see a significant improvement in disturbance rejection compared with observer-based feedback control.

We cannot achieve the goal of completely eliminating the disturbances that cause lateral motion in a web system. However, by using the strategies of repetitive control and internal model principle, we can significantly reduce the lateral motion.

Appendices

A.1 Derivation of Web PDE

The PDE that governs the lateral displacement of a web can be derived by an application of Hamilton's principle. The details on how to apply the principle is on pages 132–135 of [21]; we follow the same procedure here.

Consider the web between two rollers as in Figure 2.3 under constant tension T along the x axis and moving at a velocity v. The kinematic energy of the web is

$$K = \frac{1}{2}\int_0^L m\left[v^2 + \left(\frac{\partial y}{\partial t} + v\frac{\partial y}{\partial x}\right)^2\right]^2 dx + \frac{1}{2}\int_0^L J\left(\frac{\partial \theta}{\partial t} + v\frac{\partial \theta}{\partial x}\right)^2 dx, \tag{1}$$

where m is the mass, J is the rotary inertia, $y(x,t)$ is the lateral displacement at position x and time t, and $\theta(x,t)$ is the angle of face rotation at position x and time t. The potential energy of the web is

$$V = \frac{1}{2}\int_0^L EI\left(\frac{\partial \theta}{\partial x}\right)^2 dx + \frac{1}{2}\int_0^L \frac{GA}{n}\left(\frac{\partial y}{\partial x} - \theta\right)^2 dx + \frac{1}{2}\int_0^L T\left(\frac{\partial y}{\partial x}\right)^2 dx, \tag{2}$$

where EI is the bending stiffness, GA is the shear stiffness, and n is a constant. With equations (1) and (2) we apply Hamilton's principle. In other words, the PDE governing the lateral displacement of the web is one that renders

$$I = \int_{t_1}^{t_2} (K - V)dt$$

an extremum with respect to $y(x,t)$ and $\theta(x,t)$, where $t_2 > t_1$. As a result, we obtain two

equations:

$$-m\left(\frac{\partial^2 y}{\partial t^2}+4v\frac{\partial^2 y}{\partial x\partial t}+v^2\frac{\partial^2 y}{\partial x^2}\right)+\left(T+\frac{GA}{n}\right)\frac{\partial^2 y}{\partial x^2}-\frac{GA}{n}\frac{\partial\theta}{\partial x}=0 \tag{3}$$

$$-J\left(\frac{\partial^2\theta}{\partial t^2}+4v\frac{\partial^2\theta}{\partial x\partial t}+v^2\frac{\partial^2\theta}{\partial x^2}\right)+EI\frac{\partial^2\theta}{\partial x^2}+\frac{GA}{n}\left(\frac{\partial y}{\partial x}-\theta\right)=0. \tag{4}$$

We now simplify equations (3) and (4) to a PDE of $y(x,t)$. This is achieved in the following way. First, we differentiate (4) with respect to x:

$$-J\left(\frac{\partial^3\theta}{\partial x\partial t^2}+4v\frac{\partial^3\theta}{\partial x^2\partial t}+v^2\frac{\partial^3\theta}{\partial x^3}\right)+EI\frac{\partial^3\theta}{\partial x^3}+\frac{GA}{n}\left(\frac{\partial^2 y}{\partial x^2}-\frac{\partial\theta}{\partial x}\right)=0. \tag{5}$$

Second, we solve equation (3) for $\frac{\partial\theta}{\partial x}$:

$$\frac{\partial\theta}{\partial x}=\frac{n}{GA}\left[-m\left(\frac{\partial^2 y}{\partial t^2}+4v\frac{\partial^2 y}{\partial x\partial t}+v^2\frac{\partial^2 y}{\partial x^2}\right)+\left(T+\frac{GA}{n}\right)\frac{\partial^2 y}{\partial x^2}\right], \tag{6}$$

and then differentiate (6)with respect to x or t or both to get $\frac{\partial^3\theta}{\partial x\partial t^2}$, $\frac{\partial^3\theta}{\partial x^2\partial t}$, and $\frac{\partial^3\theta}{\partial x^3}$:

$$\frac{\partial^3\theta}{\partial x\partial t^2}=\frac{n}{GA}\left[-m\left(\frac{\partial^4 y}{\partial t^4}+4v\frac{\partial^4 y}{\partial x\partial t^3}+v^2\frac{\partial^4 y}{\partial x^2\partial t^2}\right)+\left(T+\frac{GA}{n}\right)\frac{\partial^4 y}{\partial x^2\partial t^2}\right] \tag{7}$$

$$\frac{\partial^3\theta}{\partial x^2\partial t}=\frac{n}{GA}\left[-m\left(\frac{\partial^4}{\partial x\partial t^3}+4v\frac{\partial^4 y}{\partial x^2\partial t^2}+v^2\frac{\partial^4 y}{\partial x^3\partial t}\right)+\left(T+\frac{GA}{n}\right)\frac{\partial^4 y}{\partial x^3\partial t}\right] \tag{8}$$

$$\frac{\partial^3\theta}{\partial x^3}=\frac{n}{GA}\left[-m\left(\frac{\partial^4 y}{\partial x^2\partial t^2}+4v\frac{\partial^4 y}{\partial x^3\partial t}+v^2\frac{\partial^4 y}{\partial x^4}\right)+\left(T+\frac{GA}{n}\right)\frac{\partial^4 y}{\partial x^4}\right]. \tag{9}$$

We substitute the equations for $\frac{\partial\theta}{\partial x}$ (6), $\frac{\partial^3\theta}{\partial x\partial t^2}$ (7), $\frac{\partial^3\theta}{\partial x^2\partial t}$ (8), and $\frac{\partial^3\theta}{\partial x^3}$(9) into equation (5) to obtain terms only in y and its derivatives:

$$\begin{aligned}0=&(Jv^2-EI)\left(\frac{nmv^2}{GA}-\frac{nT}{GA}-1\right)\frac{\partial^4 y}{\partial x^4}+(mv^2-T)\frac{\partial^2 y}{\partial x^2}+4mv\frac{\partial^2 y}{\partial x\partial t}+m\frac{\partial^2 y}{\partial t^2}\\&+\left(\frac{18Jnmv^2}{GA}-\frac{EInm}{GA}-\frac{JnT}{GA}-J\right)\frac{\partial^4 y}{\partial x^2\partial t^2}+\frac{Jnm}{GA}\frac{\partial^4 y}{\partial t^4}+\frac{8Jnmv}{GA}\frac{\partial^4 y}{\partial x\partial t^3}\\&+\left(\frac{8Jnmv^3}{GA}-\frac{4EInmv}{GA}-\frac{4JnTv}{GA}-4Jv\right)\frac{\partial^4 y}{\partial x^3\partial t}.\end{aligned}$$

The expression for the boundary condition θ can be derived as follows. First, we differentiate equation (6) to get $\frac{\partial^2\theta}{\partial x^2}$:

$$\frac{\partial^2\theta}{\partial x^2} = \frac{n}{GA}\left[-m\left(\frac{\partial^3 y}{\partial x \partial t^2} + 4v\frac{\partial^3 y}{\partial x^2 \partial t} + v^2\frac{\partial^3 y}{\partial x^3}\right) + \left(T + \frac{GA}{n}\right)\frac{\partial^3 y}{\partial x^3}\right]. \tag{10}$$

Second, we substitute the equation for $\frac{\partial^2\theta}{\partial x^2}$ (10) into equation (4) and then use the two assumptions: 1) $T \gg mv^2$; 2) $EI \gg Jv^2$ to get an expression for θ in terms of y and its derivatives:

$$\theta = \frac{\partial y}{\partial x} + EI\frac{n}{GA}\left(1 + \frac{nT}{GA}\right)\frac{\partial^3 y}{\partial x^3}.$$

A.2 Derivation of State-Space Form

The derivation of the state-space form from the system dynamics can be found on pages 102–111 of [4]. We offer a slightly different derivation using notation from Chapter 2.

The lateral displacement of the web is

$$y(x,t) = y_{i-1}(t)X_1(x) + \theta_{i-1}(t)X_2(x) + y_i(t)X_3(x) + \theta_i(t)X_4(x), \qquad i = 1,\ldots,4, \tag{11}$$

where $X_i(x)$ are defined in equations (2.16) in Chapter 2. The web slope and curvature of roller R_i are respectively

$$\frac{\partial y_i}{\partial x} = y_{i-1}X_1'(L_i) + \theta_{i-1}X_2'(L_i) + y_iX_3'(L_i) + \theta_iX_4'(L_i) \tag{12}$$

$$\frac{\partial^2 y_i}{\partial x^2} = y_{i-1}X_1''(L_i) + \theta_{i-1}X_2''(L_i) + y_iX_3''(L_i) + \theta_iX_4''(L_i). \tag{13}$$

We solve for θ_i in the web slope equation (12):

$$\theta_i = \frac{1}{X_4'(L_i)}\left(\frac{\partial y_i}{\partial x} - y_{i-1}X_1'(L_i) + \theta_{i-1}X_2'(L_i) + y_iX_3'(L_i)\right), \tag{14}$$

and then substitute it into the web curvature equation (13):

$$\begin{aligned}\frac{\partial^2 y_i}{\partial x^2} &= y_{i-1}X_1''(L_i) + \theta_{i-1}X_2''(L_i) + y_i X_3''(L_i) \\ &\quad + \frac{X_4''(L_i)}{X_4'(L_i)}\left(\frac{\partial y_i}{\partial x} - y_{i-1}X_1'(L_i) + \theta_{i-1}X_2'(L_i) + y_i X_3'(L_i)\right) \\ &= y_{i-1}\left(X_1''(L_i) - \frac{X_1'(L_i)X_4''(L_i)}{X_4'(L_i)}\right) + \theta_{i-1}\left(X_2''(L_i) - \frac{X_2'(L_i)X_4''(L_i)}{X_4'(L_i)}\right) \\ &\quad + y_i\left(X_3''(L_i) - \frac{X_3'(L_i)X_4''(L_i)}{X_4'(L_i)}\right) + \frac{\partial y_i}{\partial x}\left(\frac{X_4''(L_i)}{X_4'(L_i)}\right) \\ &= y_{i-1}W_1(L_i) + \theta_{i-1}W_2(L_i) + y_i W_3(L_i) + \frac{\partial y_i}{\partial x}W_4(L_i), \end{aligned} \tag{15}$$

where W_1, W_2, W_3, and W_4 are defined by

$$W_1(L_i) = X_1''(L_i) - \frac{X_1'(L_i)X_4''(L_i)}{X_4'(L_i)}, \qquad W_2(L_i) = X_2''(L_i) - \frac{X_2'(L_i)X_4''(L_i)}{X_4'(L_i)},$$
$$W_3(L_i) = X_3''(L_i) - \frac{X_3'(L_i)X_4''(L_i)}{X_4'(L_i)}, \qquad W_4(L_i) = \frac{X_4''(L_i)}{X_4'(L_i)}.$$

We can use the web slope and web curvature expressions in (12) and (15) in the dynamics.

The system dynamics are

$$\frac{dy_1}{dt} = -v\frac{\partial y_1}{\partial x}, \tag{16}$$
$$\frac{d^2 y_1}{dt^2} = v^2\frac{\partial^2 y_1}{\partial x^2}, \tag{17}$$
$$\frac{dy_2}{dt} = v\left(\frac{z_2}{L_2} - \frac{\partial y_2}{\partial x}\right) + \frac{dz_2}{dt}, \tag{18}$$
$$\frac{d^2 y_2}{dt^2} = v^2\frac{\partial^2 y_2}{\partial x^2} + \frac{d^2 z_2}{dt^2}, \tag{19}$$
$$\frac{dy_3}{dt} = -v\frac{\partial y_3}{\partial x}, \tag{20}$$
$$\frac{d^2 y_3}{dt^2} = v^2\frac{\partial^2 y_3}{\partial x^2}, \tag{21}$$
$$\frac{dy_4}{dt} = -v\frac{\partial y_4}{\partial x}, \tag{22}$$
$$\frac{d^2 y_4}{dt^2} = v^2\frac{\partial^2 y_4}{\partial x^2}. \tag{23}$$

If we choose the state x, output y, control input u, and disturbance w as

$$x = \begin{bmatrix} y_1 & \frac{dy_1}{dt} & y_2 & \frac{dy_2}{dt} & y_3 & \frac{dy_3}{dt} & y_4 & \frac{dy_4}{dt} & z_2 & \frac{dz_2}{dt} \end{bmatrix}^T,$$

$$y(t) = y_2(t), \qquad u(t) = \frac{d^2 z_2(t)}{dt^2}, \qquad w(t) = \begin{bmatrix} y_0(t) & \theta_0(t) \end{bmatrix}^T,$$

then the state-space form can be derived as follows. The remainder of the derivation uses the interchangeable notation $\dot{x}$ and $\frac{dx}{dt}$ to represent the time derivative.

$\mathbf{x_1}$: $x_1 = y_1 \Rightarrow \dot{x_1} = \frac{dy_1}{dt} = x_2$.

$\mathbf{x_2}$: $x_2 = \frac{dy_1}{dt} \Rightarrow \dot{x_2} = \frac{d^2 y_1}{dt} = v^2 \frac{\partial^2 y_1}{\partial x^2}$

$$\dot{x_2} = v^2 \left(y_0 W_1(L_1) + \theta_0 W_2(L_1) + y_1 W_3(L_1) + \frac{\partial y_1}{\partial x} W_4(L_1) \right) \tag{24}$$

where web curvature equation (15) with $i = 1$ is used to get equation (24). We then solve the velocity equation (16) for $\frac{\partial y_1}{\partial x}$:

$$\frac{\partial y_1}{\partial x} = -\frac{1}{v} \frac{dy_1}{dt},$$

so that $\dot{x_2}$ can be simplified to state-space variables:

$$\begin{aligned} \dot{x_2} &= v^2 W_3(L_1) y_1 - v W_4(L_1) \frac{dy_1}{dt} + v^2 W_1(L_1) y_0 + v^2 W_2(L_1) \theta_0 \\ &= v^2 W_3(L_1) x_1 - v W_4(L_1) x_2 + v^2 W_1(L_1) y_0 + v^2 W_2(L_1) \theta_0. \end{aligned}$$

$\mathbf{x_3}$: $x_3 = y_2 \Rightarrow \dot{x_3} = \frac{dy_2}{dt} = x_4$.

$\mathbf{x_4}$: $x_4 = \frac{dy_2}{dt} \Rightarrow \dot{x_4} = \frac{d^2 y_2}{dt^2} = v^2 \frac{\partial^2 y_2}{\partial x^2} + \frac{d^2 z_2}{dt^2}$

$$\dot{x_4} = v^2 \left(y_1 W_1(L_2) + \theta_1 W_2(L_2) + y_2 W_3(L_2) + \frac{\partial y_2}{\partial x} W_4(L_2) \right), \tag{25}$$

where web curvature equation (15) with $i = 2$ is used to get equation (25). We then use equation (14) with $i = 1$ for θ_1:

$$\theta_1 = \frac{1}{X_4'(L_1)} \left(\frac{\partial y_1}{\partial x} - y_0 X_1'(L_1) - \theta_0 X_2'(L_1) - y_1 X_3'(L_1) \right),$$

and solve the velocity equation (18) for $\frac{\partial y_2}{\partial x}$:

$$\frac{\partial y_2}{\partial x} = -\frac{1}{v}\left(\frac{dy_2}{dt} - \frac{dz_2}{dt}\right) + \frac{z_2}{L_2},$$

so that $\dot{x_4}$ can be simplified to state-space variables:

$$\begin{aligned}
\dot{x_4} &= \left(v^2 W_1(L_2) - v^2 W_2(L_2)\frac{X_3'(L_1)}{X_4'(L_1)}\right) y_1 + v^2 W_3(L_2) y_2 \\
&\quad + v^2 W_4(L_2)\left[\frac{z_2}{L_2} - \frac{1}{v}\left(\frac{dy_2}{dt} - \frac{dz_2}{dt}\right)\right] \\
&\quad + v^2 \frac{W_2(L_2)}{X_4'(L_1)}\left(-\frac{1}{v}\frac{dy_1}{dt} - X_1'(L_1) y_0 - X_2'(L_1)\theta_0\right) + \frac{d^2 z_2}{dt^2} \\
&= \left(v^2 W_1(L_2) - v^2 W_2(L_2)\frac{X_3'(L_1)}{X_4'(L_1)}\right) x_1 - v\frac{W_2(L_2)}{X_4'(L_1)} x_2 + v^2 W_3(L_2) x_3 \\
&\quad - v W_4(L_2) x_4 + \frac{v^2 W_4(L_2)}{L_2} x_9 + v W_4(L_2) x_{10} \\
&\quad - v^2 \frac{W_2(L_2)}{X_4'(L_1)}\left(X_1'(L_1) y_0 + X_2'(L_1)\theta_0\right) + u.
\end{aligned}$$

$\mathbf{x_5}$: $x_5 = y_3 \Rightarrow \dot{x_5} = \frac{dy_3}{dt} = x_6$.

$\mathbf{x_6}$: $x_6 = \frac{dy_3}{dt} \Rightarrow \dot{x_6} = \frac{d^2 y_3}{dt^2} = v^2 \frac{\partial^2 y_3}{\partial x^2}$

$$\dot{x_6} = v^2\left(y_2 W_1(L_3) + \theta_2 W_2(L_3) + y_3 W_3(L_3) + \frac{\partial y_3}{\partial x} W_4(L_3)\right), \tag{26}$$

where web curvature equation (15) with $i = 3$ is used to get equation (26). We then use equation (14) with $i = 2$ and back-solve for θ_2:

$$\begin{aligned}
\theta_2 &= \frac{1}{X_4'(L_2)}\left(\frac{\partial y_2}{\partial x} - y_1 X_1'(L_2) - \theta_1 X_2'(L_2) - y_2 X_3'(L_2)\right) \\
\theta_2 &= \frac{1}{X_4'(L_2)}\left[\frac{\partial y_2}{\partial x} + \left(\frac{X_2'(L_2) X_3'(L_1)}{X_4'(L_1)} - X_1'(L_2)\right) y_1 - X_3'(L_2) y_2\right] \\
&\quad - \frac{X_2'(L_2)}{X_4'(L_2) X_4'(L_1)}\left(\frac{\partial y_1}{\partial x} - X_1'(L_1) y_0 - X_2'(L_1)\theta_0\right),
\end{aligned}$$

and solve the velocity equation (20) for $\frac{\partial y_3}{\partial x}$:

$$\frac{\partial y_3}{\partial x} = -\frac{1}{v}\frac{dy_3}{dt},$$

so that $\dot{x_6}$ can be simplified to state-space variables:

$$\begin{aligned}
\dot{x_6} &= \left(v^2 W_1(L_3) - v^2 \frac{W_2(L_3)X_3'(L_2)}{X_4'(L_2)}\right) y_2 + v^2 W_3(L_3) y_3 - v W_4(L_3)\frac{dy_3}{dt} \\
&\quad + v^2 \frac{W_2(L_3)}{X_4'(L_2)}\left[-\frac{1}{v}\left(\frac{dy_2}{dt} - \frac{dz_2}{dt}\right) + \frac{z_2}{L_2} + \left(\frac{X_2'(L_2)X_3'(L_1)}{X_4'(L_1)} - X_1'(L_2)\right) y_1\right] \\
&\quad + v^2 \frac{W_2(L_3)}{X_4'(L_2)}\frac{X_2'(L_2)}{X_4'(L_1)}\left(\frac{1}{v}\frac{dy_1}{dt} + X_1'(L_1)y_0 + X_2'(L_1)\theta_0\right) \\
&= v^2 \frac{W_2(L_3)}{X_4'(L_2)}\left(\frac{X_2'(L_2)X_3'(L_1)}{X_4'(L_1)} - X_1'(L_2)\right) x_1 + v\frac{W_2(L_3)}{X_4'(L_2)}\frac{X_2'(L_2)}{X_4'(L_1)} x_2 \\
&\quad + \left(v^2 W_1(L_3) - v^2 \frac{W_2(L_3)X_3'(L_2)}{X_4'(L_2)}\right) x_3 - v\frac{W_2(L_3)}{X_4'(L_2)} x_4 + v^2 W_3(L_3) x_5 - v W_4(L_3) x_6 \\
&\quad + v^2 \frac{W_2(L_3)}{X_4'(L_2)}\frac{1}{L_2} x_9 + v\frac{W_2(L_3)}{X_4'(L_2)} x_{10}.
\end{aligned}$$

$\mathbf{x_7}$: $x_7 = y_4 \Rightarrow \dot{x_7} = \frac{dy_4}{dt} = x_8$.

$\mathbf{x_8}$: $x_8 = \frac{dy_4}{dt} \Rightarrow \dot{x_8} = \frac{d^2 y_4}{dt^2} = v^2 \frac{\partial^2 y_4}{\partial x^2}$

$$\dot{x_8} = v^2\left(y_3 W_1(L_4) + \theta_3 W_2(L_4) + y_4 W_3(L_4) + \frac{\partial y_4}{\partial x} W_4(L_4)\right), \tag{27}$$

where web curvature equation (15) with $i = 4$ is used to get equation (27). We then use equation (14) with $i = 3$ and back-solve for θ_3:

$$\begin{aligned}
\theta_3 &= \frac{1}{X_4'(L_3)}\left(\frac{\partial y_3}{\partial x} - y_2 X_1'(L_3) - \theta_2 X_2'(L_3) - y_3 X_3'(L_3)\right) \\
&= \frac{1}{X_4'(L_3)}\left(\frac{\partial y_3}{\partial x} - y_2 X_1'(L_3) - y_3 X_3'(L_3)\right) \\
&\quad - \frac{1}{X_4'(L_3)}\frac{X_2'(L_3)}{X_4'(L_2)}\left[\frac{\partial y_2}{\partial x} + \left(\frac{X_2'(L_2)X_3'(L_1)}{X_4'(L_1)} - X_1'(L_2)\right) y_1 - X_3'(L_2) y_2\right] \\
&\quad - \frac{1}{X_4'(L_3)}\frac{X_2'(L_3)}{X_4'(L_2)}\frac{X_2'(L_2)}{X_4'(L_1)}\left(\frac{\partial y_1}{\partial x} - X_1'(L_1)y_0 - X_2'(L_1)\theta_0\right),
\end{aligned}$$

and solve the velocity equation (22) for $\frac{\partial y_4}{\partial x}$:

$$\frac{\partial y_4}{\partial x} = -\frac{1}{v}\frac{dy_4}{dt},$$

so that $\dot{x_8}$ can be simplified to state-space variables:

$$\begin{aligned}
\dot{x_8} &= v^2 W_1(L_4) y_3 + v^2 W_3(L_4) y_4 - v W_4(L_4)\frac{dy_4}{dt} \\
&\quad + v^2 \frac{W_2(L_4)}{X_4'(L_3)}\left[-\frac{1}{v}\frac{dy_3}{dt} + \left(\frac{X_2'(L_3)}{X_4'(L_2)} - X_1'(L_3)\right) y_2 - X_3'(L_3) y_3\right] \\
&\quad - v^2 \frac{W_2(L_4)}{X_4'(L_3)}\frac{X_2'(L_3)}{X_4'(L_2)}\left[-\frac{1}{v}\left(\frac{dy_2}{dt} - \frac{dz_2}{dt}\right) + \frac{z_2}{L_2} + \left(\frac{X_2'(L_2)X_3'(L_1)}{X_4'(L_1)} - X_1'(L_2)\right) y_1\right] \\
&\quad + v^2 \frac{W_2(L_4)}{X_4'(L_3)}\frac{X_2'(L_3)}{X_4'(L_2)}\frac{X_2'(L_2)}{X_4'(L_1)}\left(-\frac{1}{v}\frac{dy_1}{dt} - X_1'(L_1) y_0 - X_2'(L_1)\theta_0\right) \\
&= -v^2 \frac{W_2(L_4)}{X_4'(L_3)}\frac{X_2'(L_3)}{X_4'(L_2)}\left(\frac{X_2'(L_2)X_3'(L_1)}{X_4'(L_1)} - X_1'(L_2)\right) x_1 - v\frac{W_2(L_4)}{X_4'(L_3)}\frac{X_2'(L_3)}{X_4'(L_2)}\frac{X_2'(L_2)}{X_4'(L_1)} x_2 \\
&\quad + v^2 \frac{W_2(L_4)}{X_4'(L_3)}\left(\frac{X_2'(L_3)}{X_4'(L_2)} - X_1'(L_3)\right) x_3 + v\frac{W_2(L_4)}{X_4'(L_3)}\frac{X_2'(L_3)}{X_4'(L_2)} x_4 \\
&\quad + \left(v^2 W_1(L_4) - v^2 \frac{W_2(L_4)X_3'(L_3)}{X_4'(L_3)}\right) x_5 - v\frac{W_2(L_4)}{X_4'(L_3)} x_6 + v^2 W_3(L_4) x_7 - v W_4(L_4) x_8 \\
&\quad - v^2 \frac{W_2(L_4)}{X_4'(L_3)}\frac{X_2'(L_3)}{X_4'(L_2)}\frac{1}{L_2} x_9 - v\frac{W_2(L_4)}{X_4'(L_3)}\frac{X_2'(L_3)}{X_4'(L_2)} x_{10}.
\end{aligned}$$

$\mathbf{x_9}$: $x_9 = z_2 \Rightarrow \dot{x_9} = \frac{dz_2}{dt} = x_{10}$.

$\mathbf{x_{10}}$: $x_{10} = \frac{dz_2}{dt} \Rightarrow \dot{x_{10}} = \frac{d^2 z_2}{dt^2} = u$.

Hence, the state-space form is given by

$$\begin{aligned}
\dot{x}(t) &= Ax(t) + Bu(t) + Fw(t) \\
y(t) &= Cx(t),
\end{aligned}$$

where $A \in \mathbb{R}^{10\times 10}$, $B \in \mathbb{R}^{10\times 1}$, $F \in \mathbb{R}^{10\times 2}$, $C \in \mathbb{R}^{1\times 10}$ are

$$A = \begin{bmatrix} 0 & 1 & 0 & 0 & 0 & 0 & 0 & 0 & 0 & 0 \\ a_{21} & a_{22} & 0 & 0 & 0 & 0 & 0 & 0 & 0 & 0 \\ 0 & 0 & 0 & 1 & 0 & 0 & 0 & 0 & 0 & 0 \\ a_{41} & a_{42} & a_{43} & a_{44} & 0 & 0 & 0 & 0 & a_{49} & a_{4,10} \\ 0 & 0 & 0 & 0 & 0 & 1 & 0 & 0 & 0 & 0 \\ a_{61} & a_{62} & a_{63} & a_{64} & a_{65} & a_{66} & 0 & 0 & a_{69} & a_{6,10} \\ 0 & 0 & 0 & 0 & 0 & 0 & 0 & 1 & 0 & 0 \\ a_{81} & a_{82} & a_{83} & a_{84} & a_{85} & a_{86} & a_{87} & a_{88} & a_{89} & a_{8,10} \\ 0 & 0 & 0 & 0 & 0 & 0 & 0 & 0 & 0 & 1 \\ 0 & 0 & 0 & 0 & 0 & 0 & 0 & 0 & 0 & 0 \end{bmatrix}$$

$$B = \begin{bmatrix} 0 & 0 & 1 & 0 & 0 & 0 & 0 & 0 & 0 & 1 \end{bmatrix}^T$$

$$C = \begin{bmatrix} 0 & 0 & 1 & 0 & 0 & 0 & 0 & 0 & 0 & 0 \end{bmatrix}$$

$$F = \begin{bmatrix} 0 & f_{21} & 0 & f_{41} & 0 & f_{61} & 0 & f_{81} & 0 & 0 \\ 0 & f_{22} & 0 & f_{42} & 0 & f_{62} & 0 & f_{82} & 0 & 0 \end{bmatrix}^T,$$

with

$$\begin{aligned} a_{21} &= v^2 W_3(L_1) \\ a_{22} &= -v W_4(L_1) \\ a_{41} &= v^2 W_1(L_2) - v^2 W_2(L_2) \frac{X_3'(L_1)}{X_4'(L_1)} \\ a_{42} &= -v \frac{W_2(L_2)}{X_4'(L_1)} \\ a_{43} &= v^2 W_3(L_2) \\ a_{44} &= -v W_4(L_2) \\ a_{49} &= \frac{v^2}{L_2} W_4(L_2) \\ a_{4,10} &= v W_4(L_2) \end{aligned}$$

$$
\begin{aligned}
a_{61} &= v^2 \frac{W_2(L_3)}{X_4'(L_2)} \left(\frac{X_2'(L_2) X_3'(L_1)}{X_4'(L_1)} - X_1'(L_2) \right) \\
a_{62} &= v \frac{W_2(L_3)}{X_4'(L_2)} \frac{X_2'(L_2)}{X_4'(L_1)} \\
a_{63} &= v^2 W_1(L_3) - v^2 \frac{W_2(L_3) X_3'(L_2)}{X_4'(L_2)} \\
a_{64} &= -v \frac{W_2(L_3)}{X_4'(L_2)} \\
a_{65} &= v^2 W_3(L_3) \\
a_{66} &= -v W_4(L_3) \\
a_{69} &= \frac{v^2}{L_2} \frac{W_2(L_3)}{X_4'(L_2)} \\
a_{6,10} &= v \frac{W_2(L_3)}{X_4'(L_2)} \\
a_{81} &= -v^2 \frac{W_2(L_4)}{X_4'(L_3)} \frac{X_2'(L_3)}{X_4'(L_2)} \left(\frac{X_2'(L_2) X_3'(L_1)}{X_4'(L_1)} - X_1'(L_2) \right) \\
a_{82} &= -v \frac{W_2(L_4)}{X_4'(L_3)} \frac{X_2'(L_3)}{X_4'(L_2)} \frac{X_2'(L_2)}{X_4'(L_1)} \\
a_{83} &= v^2 \frac{W_2(L_4)}{X_4'(L_3)} \left(\frac{X_2'(L_3)}{X_4'(L_2)} - X_1'(L_3) \right) \\
a_{84} &= v \frac{W_2(L_4)}{X_4'(L_3)} \frac{X_2'(L_3)}{X_4'(L_2)} \\
a_{85} &= v^2 W_1(L_4) - v^2 \frac{W_2(L_4) X_3'(L_3)}{X_4'(L_3)} \\
a_{86} &= -v \frac{W_2(L_4)}{X_4'(L_3)} \\
a_{87} &= v^2 W_3(L_4) \\
a_{88} &= -v W_4(L_4) \\
a_{89} &= -\frac{v^2}{L_2} \frac{W_2(L_4)}{X_4'(L_3)} \frac{X_2'(L_3)}{X_4'(L_2)} \\
a_{8,10} &= -v \frac{W_2(L_4)}{X_4'(L_3)} \frac{X_2'(L_3)}{X_4'(L_2)}
\end{aligned}
$$

$$
\begin{aligned}
f_{21} &= v^2 W_1(L_1) \\
f_{22} &= v^2 W_2(L_1) \\
f_{41} &= -v^2 \frac{W_2(L_2) X_1'(L_1)}{X_4'(L_1)} \\
f_{42} &= -v^2 \frac{W_2(L_2) X_2'(L_1)}{X_4'(L_1)} \\
f_{61} &= v^2 \frac{W_2(L_3)}{X_4'(L_2)} \frac{X_2'(L_2) X_1'(L_1)}{X_4'(L_1)} \\
f_{62} &= v^2 \frac{W_2(L_3)}{X_4'(L_2)} \frac{X_2'(L_2) X_2'(L_1)}{X_4'(L_1)} \\
f_{81} &= -v^2 \frac{W_2(L_4)}{X_4'(L_3)} \frac{X_2'(L_3)}{X_4'(L_2)} \frac{X_2'(L_2) X_1'(L_1)}{X_4'(L_1)} \\
f_{82} &= -v^2 \frac{W_2(L_4)}{X_4'(L_3)} \frac{X_2'(L_3)}{X_4'(L_2)} \frac{X_2'(L_2) X_2'(L_1)}{X_4'(L_1)}.
\end{aligned}
$$

A.3 Nomenclature and Simulation Values

Table 1: Nomenclature

Variable	Description
T	tension in the web
EI	Young's modulus times moment of inertia (bending stiffness)
GA	shear modulus times cross sectional area (shear stiffness)
v	velocity of the web
n	constant in beam model
m	mass of the web
$\frac{\partial y}{\partial x}$	web slope
$\frac{\partial^2 y}{\partial x^2}$	web curvature
γ	pivot angle of the displacement guide
z	lateral displacement of the guide
$\frac{dz}{dt}$	lateral velocity of the guide
$\frac{d^2 z}{dt^2}$	lateral acceleration of the guide
J	rotary inertia
L_1	distance between rollers R_0 and R_1
L_2	distance between rollers R_1 and R_2
L_3	distance between rollers R_2 and R_3
L_4	distance between rollers R_3 and R_4

Table 2: Simulation Values

Variable	Imperial units	SI units
T	20 lb_f	89 N
EI	1.76×10^8 $\text{lb}_f \cdot \text{in}^2$	5.05×10^5 $\text{N} \cdot \text{m}^2$
GA	3.42×10^5 lb_f	1.52×10^6 N
v	40 in/s	1.02 m/s
n	1	1
L_1	29 in	0.74 m
L_2	22 in	0.56 m
L_3	40 in	1.02 m
L_4	61 in	1.55 m

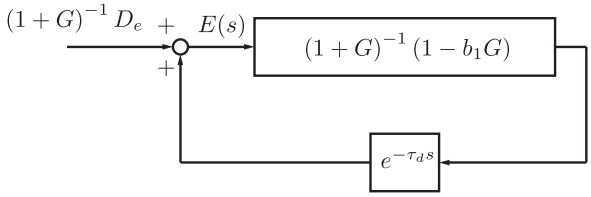

Figure 1: System in block form.

A.4 Stability of Repetitive Controller

Consider the system

$$E(s) = e^{-\tau_d s}\left(1+G(s)\right)^{-1}\ \left(1-b_1(s)G(s)\right)E(s) + \left(1+G(s)\right)^{-1}D_e(s), \tag{28}$$

where

$$D_e(s) = \left(1-e^{-\tau_d s}\right)\left(-D(s)-\bar{Y}(s)\right) - G(s)\bar{W}(s).$$

System (28) can be represented by Figure 1. We use the small gain theorem to show BIBO stability; that is, if we can show that $(1+G)^{-1}D_e$ is an $\mathbf{L_2}$ function, and the loop gain is less than one, then we can conclude that the system is BIBO stable [9]. Here we define an $\mathbf{L_2}$ function to be one that satisfies $\int_0^\infty e(t)e(t)dt < \infty$.

Proposition 1 (Proposition 1 of [9])**.** *Given the system shown in Figure 1, where $G(s)$ is a strictly proper transfer function, $b_1(s)$ is a stable proper transfer function, and $d(t)$ is bounded continuous periodic with period τ_d. If*

1) $(1+G(s))^{-1}G(s)$ *is asymptotically stable,*

2) $\|(1+G(s))^{-1}(1-b_1(s)G(s))\|_\infty < 1$,

then $e(t) \in \mathbf{L_2}$.

Proof. First, we show that $(1+G)^{-1}D_e$ is an $\mathbf{L_2}$ under the assumption of condition 1. The function

$$\begin{aligned}\mathcal{L}^{-1}\left[(1-e^{-\tau_d s})D(s)\right] &= \mathcal{L}^{-1}\left[\int_0^L e^{-st}d(t)dt\right] \\ &= \begin{cases} d(t), & 0 \le t \le L \\ 0, & t > L, \end{cases}\end{aligned}$$

is $\mathbf{L_2}$. Observe that $(1+G)^{-1}$ is stable in view of $(1+G)^{-1}G$ being stable since $(1+G)^{-1} = 1-(1+G)^{-1}G$. Thus, the functions

$$\mathcal{L}^{-1}\left[(1+G)^{-1}(1-e^{-\tau_d s})\bar{Y}\right]$$
$$\mathcal{L}^{-1}\left[(1+G)^{-1}G\bar{W}\right]$$

are also $\mathbf{L_2}$, meaning that the input $(1+G)^{-1}D_e$ is an $\mathbf{L_2}$ function. Also, we see that $(1+G)^{-1}(1-b_1G)$ is stable as well. Since the induced $\mathbf{L_2}$ norm is [22]

$$\begin{aligned}\|(1+G)^{-1}(1-b_1G)\|_2 &= \sup_{\omega}|(1+G)^{-1}(1-b_1G)| \\ &= \|1+G)^{-1}(1-b_1G)\|_\infty,\end{aligned}$$

and $|e^{-j\omega\tau_d}| = 1$, the result follows from the small gain theorem [22]. □

A.5 Stability Theorem

Theorem 4 (Theorem on p. 176 in [23]). *Assume the poles of the closed-loop system are given in the form:*

$$X(s) + \sum_{i=1}^{m} Z_i(s)e^{-\tau_i s},$$

where

$$X(s) = s^n + \sum_{k=0}^{n-1} a_k s^k, \qquad Z_i(s) = \sum_{k=0}^{n} b_{ki}s^n$$

with $\sum_{i=1}^{m}|b_{ni}| < 1$. *If*

1. *all roots of* $X(s)$ *have negative real parts,*
2. *for any* $\omega \geq 0$, *the following inequality is satisfied:*

$$\sum_{i=1}^{m}|Z_i(j\omega)| < |X(j\omega)|,$$

then the system is asymptotically stable.

References

[1] W. Zhou, *Robust and decentralized control of web winding systems*, Ph.D. thesis, Cleveland State University, November 2007.

[2] J. J. Shelton, *Lateral Dynamics of a Moving Web*, Ph.D. thesis, Oklahoma State University, Stillwater, OK, 1968.

[3] L.A. Sievers, M.J. Balas, and A. von Flotow, "Modeling of web conveyance systems for multivariable control," *IEEE Transactions on Automatic Control*, vol. 33, no. 6, pp. 524–531, June 1988.

[4] L.A. Sievers, *Modeling and Control of Lateral Web Dynamics*, Ph.D. thesis, Rensselaer Polytechnic Institute, Troy, NY, 1987.

[5] J.B. Yerashunas, J.A. De Abreu-Garcia, and T.T. Hartley, "Control of lateral motion in moving webs," *Control Systems Technology, IEEE Transactions on*, vol. 11, no. 5, pp. 684 – 693, sept. 2003.

[6] A. Seshadri and P.R. Pagilla, "Optimal web guiding," *Journal of Dynamic Systems, Measurement, and Control*, vol. 132, no. 6, January 2010.

[7] Z. Jin, D. E. Chang, K.-H. Choi, D.-S. Kim, and J. Jo, "Stabilization of the lateral dynamics of a roll-to-roll web system," in *Electrical and Computer Engineering (CCECE), 2011 24th Canadian Conference on*, may 2011, pp. 000799 –000802.

[8] K.-H. Shin, S.-O. Kwon, S.-H. Kim, and S.-H. Song, "Feedforward control of the lateral position of a moving web using system identification," *IEEE Transactions on Industry Applications*, vol. 40, no. 6, pp. pp. 1637–1643, 2004.

[9] S. Hara, Y. Yamamoto, T. Omata, and M. Nakano, "Repetitive control system: A new type servo system for periodic exogenous signals," *IEEE Transactions on Automatic Control*, vol. 33, no. 7, pp. 659–668, July 1988.

[10] K. Srinivasan and F.-R. Shaw, "Analysis and design of repetitive control systems using the regeneration spectrum," in *American Control Conference, 1990*, may 1990, pp. 1150 –1155.

[11] J.-H. Moon, M.-N. Lee, and M.J. Chung, "Repetitive control for the track-following servo system of an optical disk drive," *Control Systems Technology, IEEE Transactions on*, vol. 6, no. 5, pp. 663 –670, sep 1998.

[12] T.-Y. Doh and M.J. Chung, "Repetitive control design for linear systems with time-varying uncertainties," *Control Theory and Applications, IEEE Proceedings* -, vol. 150, no. 4, pp. 427 – 432, july 2003.

[13] B. A. Güvenç and L. Güvenç, "Robust repetitive controller design in parameter space," *Journal of Dynamic Systems, Measurement, and Control*, vol. 128, no. 2, pp. 406–413, 2006.

[14] S. S. Garimella and K. Srinivasan, "Application of repetitive control to eccentricity compensation in rolling," *Journal of Dynamic Systems, Measurement, and Control*, vol. 118, no. 4, pp. 657–664, 1996.

[15] Li Cuiyan, Zhang Dongchun, and Zhuang Xianyi, "A survey of repetitive control," in *Intelligent Robots and Systems, 2004. (IROS 2004). Proceedings. 2004 IEEE/RSJ International Conference on*, sept.-2 oct. 2004, vol. 2, pp. 1160 – 1166 vol.2.

[16] C.-T. Chen, *Linear System Theory and Design*, Oxford University Press, Inc., New York, NY, USA, 3rd edition, 1998.

[17] B. Friedland, *Control System Design*, Dover Publications Inc., Mineola, NY, 2005.

[18] N.S. Nise, *Control Systems Engineering*, John Wiley & Sons, Inc., 5th edition, 2006.

[19] L. Qiu and K. Zhou, *Introduction to Feedback Control*, Prentice Hall, N. J., 2010.

[20] H. Kwakernaak and R. Sivan, *Linear Optimal Control Systems*, John Wiley & Sons, Inc., 1972.

[21] R. Weinstock, *Calculus of Variations With Applications to Physics and Engineering*, International Series in Pure and Applied Mathematics. McGraw Hill Book Company Inc., 1952.

[22] C. A. Desoer and M. Vidyasagar, *Feedback Systems Input-Ouput Properties*, SIAM, 2009.

[23] L.E. El'sgol'ts, S.B. Norkin, and translated by J.L. Casti, *Introduction to the Theory and Application of Differential Equations with Deviating Arguments*, Academic Press, 1973.